Sex Plant Reprod (2005) 17: 219–241
DOI 10.1007/s00497-004-0231-y

ORIGINAL ARTICLE

Paul M. Sanders · Anhthu Q. Bui · Brandon H. Le
Robert B. Goldberg

Differentiation and degeneration of cells that play a major role in tobacco anther dehiscence

Received: 14 July 2004 / Accepted: 22 August 2004 / Published online: 19 October 2004

Abstract Dehiscence is the terminal step in anther development that releases pollen grains from the wall of each theca at a specific site between the two locules. In tobacco, two groups of cells—the circular cell cluster and the stomium—are required for anther dehiscence and define the position at which pollen is released. The processes responsible for the differentiation of the circular cell cluster and the stomium from cells in specific anther regions are unknown. Nor is it understood what initiates the programmed degeneration of these cell types that ultimately is responsible for pollen release from the anther. We characterized stomium and circular cell cluster differentiation and degeneration using both light and transmission electron microscopy throughout anther development, from the emergence of stamen primordia to anther dehiscence at flower opening. We observed that histological changes within primordium L1 and L2 cells destined to become the stomium and circular cell cluster occur at the same time after the differentiation of surrounding locule regions. Sub-epidermal cells that differentiate into the circular cell cluster divide, enlarge, and generate vacuoles with calcium oxalate crystals prior to any detectable changes in prestomium epidermal cells. Differentiation and division of cells that generate the stomium occur after cell degeneration initiates in the circular cell cluster. Prior to dehiscence, the stomium consists of a small set of cytoplasmically dense cells that are easily distinguished from their larger, highly vacuolate epidermal neighbors. Plasmodesmata connections within and between cells of the stomium and circular cell cluster were observed at different developmental stages, suggesting that these cells communicate with each other. Circular cell cluster and stomium cell death is programmed developmentally and occurs at different times. Degeneration of the circular cell cluster occurs first, contributes to the formation of a bilocular anther, and generates the site of anther wall breakage. The stomium cell death process is complete at flower opening and provides an opening for pollen release from each theca. We used laser capture microdissection and real-time quantitative reverse-transcription polymerase chain reactions to demonstrate that stomium cells can be isolated from developing anthers and studied for the presence of specific mRNAs. Our data suggest that a cascade of unique gene expression events throughout anther development is required for the dehiscence program, and that the differentiation of the stomium and circular cell cluster in the interlocular region of the anther probably involves cell signaling processes.

Keywords Tobacco · Anther dehiscence · Stomium · Circular cell cluster · Laser capture microdissection

P. M. Sanders · A. Q. Bui · B. H. Le · R. B. Goldberg (✉)
Department of Molecular, Cell,
and Developmental Biology,
University of California,
Los Angeles, CA 90095–1606, USA
E-mail: bobg@ucla.edu
Tel.: +1-310-8259093
Fax: +1-310-8258201

Present address: P. M. Sanders
AgriGenesis Biosciences, One Fox Street,
P.O. Box 50, Auckland, New Zealand

Introduction

Dehiscence is the process that results in release of pollen grains from the anther at flower opening (Keijzer 1987; Bonner and Dickinson 1989; Goldberg et al. 1993; Beals and Goldberg 1997; Scott et al. 2004). In most flowering plants, the anther wall breaks along the lateral side of each anther half, or theca, within an indentation formed between the two locules (Fig. 1)—a region referred to as either the anther notch (Goldberg et al. 1995; Beals and Goldberg 1997; Sanders et al. 2000) or the stomial groove (D'Arcy 1996). In tobacco and other solanaceous plants (D'Arcy et al. 1996), two specialized cell types are found within the notch region: the stomium and the circular cell cluster (Fig. 1; Koltunow et al. 1990;

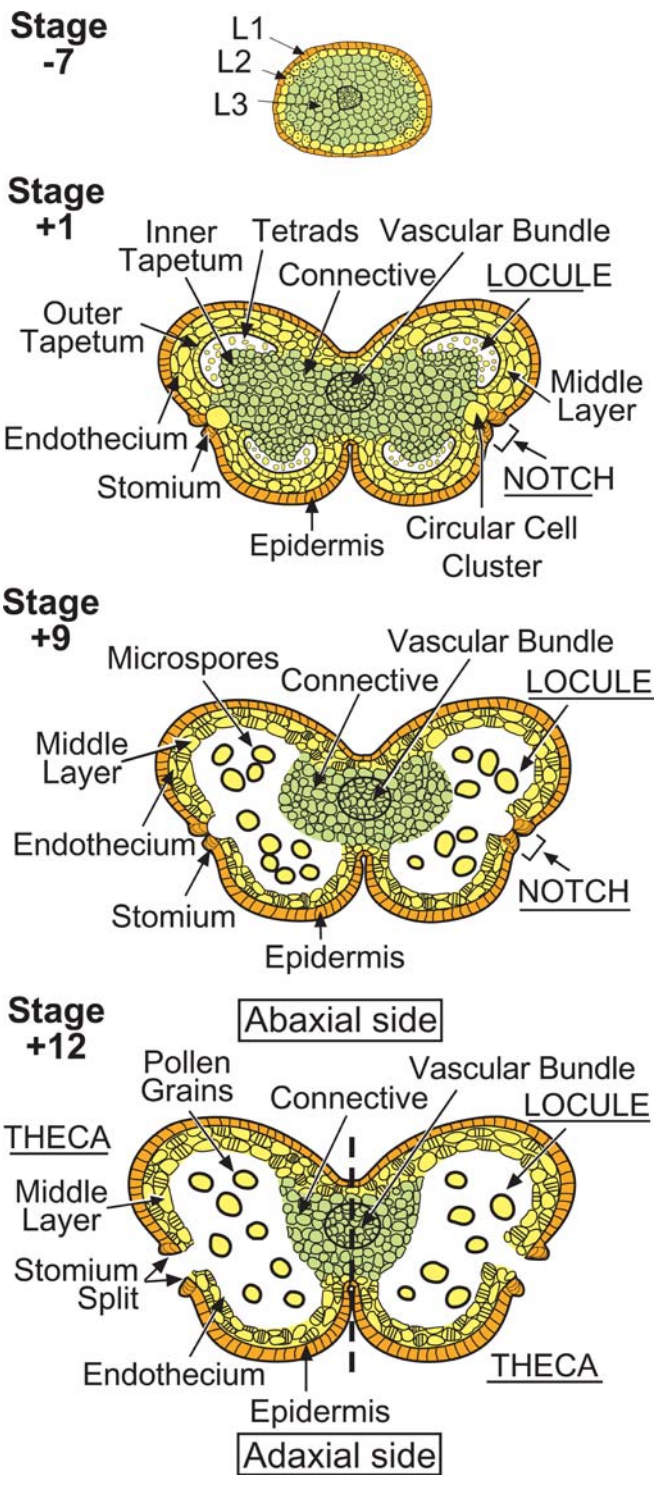

Fig. 1 Schematic representation of tobacco anther development based upon histological studies at the light microscope level (Satina and Blakeslee 1941; Joshi et al. 1967; Koltunow et al. 1990). The stages of anther development were previously described in Koltunow et al. (1990; phase 1, stages −7 to −1; phase 2, stage +1 to +12). The colors depict cells derived from the L1, L2 and L3 primordial layers at different stages of anther development (modified from Goldberg et al. 1993, 1995). In the tobacco anther, the inner middle layer is crushed during meiosis. The outer middle layer contributes to the anther wall, expands, and acquires fibrous bands similar to the endothecium. At stage +12, the *dotted line* dissects the anther in half to indicate the two theca. The two cell-types of the anther notch, the stomium and the circular cell cluster, span the length of the anther and are longitudinal columns of cells. The adaxial side of the anther is towards the center of the flower and faces the pistil. The abaxial side of the anther is outwards from the center of the flower and faces the petals

Goldberg et al. 1993, 1995; Beals and Goldberg 1997). The stomium is a specialized set of epidermal cells that degenerate and break at flower opening to allow pollen grains to be released (Fig. 1). In contrast, the circular cell cluster consists of highly specialized sub-epidermal cells that accumulate calcium oxalate crystals (Horner and Wagner 1980, 1992; Trull et al. 1991; D'Arcy et al. 1996; Iwano et al. 2004) and participate in the cell-death process that ultimately unites both locules of each theca into one large pollen chamber (Fig. 1; Koltunow et al. 1990; Goldberg et al. 1993, 1995; Beals and Goldberg 1997). The circular cell cluster has also been referred to as the intersporangial septum (Bonner and Dickinson 1989), hypodermal stomium (Horner and Wagner 1992), and oxalate package (D'Arcy et al. 1996). Recently, it has been shown that the calcium stored within the circular cell cluster becomes associated with pollen grains after circular cell cluster degeneration and facilitates the pollination process (Iwano et al. 2004). Anthers of most non-solanaceous plants (D'Arcy et al. 1996), including *Arabidopsis thaliana* (Sanders et al. 1999, 2000), do not have a circular cell cluster. However, specialized septum cells in the notch region of these anthers function analogously in dehiscence and, after their degeneration, unite the two locules of each theca into a confluent chamber (Venkatesh 1957; D'Arcy et al. 1996; Sanders et al. 2000). Neither the specification events that position the stomium and circular cell cluster in the territory between the developing anther locules, nor the mechanisms that control and coordinate their differentiation and degeneration, are known.

Tobacco anther development, including the dehiscence program, occurs in two phases (Table 1; Koltunow et al. 1990; Goldberg et al. 1993). In phase 1 (Table 1, stages −7 to −1; Koltunow et al. 1990), differentiation events establish the four locules and the stereotyped pattern of cell types that originate from the L1, L2, and L3 cell layers of the primordium (Fig. 1, stage −7) and that are present in the mature anther (Fig. 1, stage +1; Satina and Blakeslee 1941; Goldberg et al. 1993; Hill and Malmberg 1996). These include stomium and circular cell cluster formation in the notch region of the expanding anther (Fig. 1, stage +1). In addition, microspore mother cells within the locules undergo meiosis to generate haploid microspores (Fig. 1, stage +1). During phase 2 (Table 1, stages +1 to +12; Koltunow et al. 1990), filament elongation occurs, anther enlargement takes place, pollen grains differentiate from microspores in each locule, fibrous bands appear in endothecial and connective cells, and cell degeneration events within the connective, circular cell

Table 1 Major events within the notch region during tobacco anther development. Stages of tobacco anther development were taken from Koltunow et al. (1990). Major events were taken from our previous studies of tobacco anther development (Koltunow et al. 1990; Beals and Goldberg 1997) and from the observations presented here. *CCC* Circular cell cluster, *MMCells* microspore mother cells. Deep refers to periclinal cell divisions that increase the number of layers of cells seen in transverse sections (Fig. 5A). Events in italics are associated with the dehiscence program

	Stage	Anther events	Circular cell cluster[a]	Stomium
Phase 1	−7	Rounded primordia; tissue differentiation initiated	Cannot distinguish	Cannot distinguish
	−6	Intense mitotic activity in four corners of primordia; invagination of inner side	Cannot distinguish	Cannot distinguish
	−5	Wall layers, including endothecium and tapetum formed; connective established	Distinguish pre-CCC cells by position; single layer of L2 cells in future notch region	Distinguish pre-stomium cells by position in L1 layer between developing locules
	−4	Tapetum and locules distinct; middle layer crushed; vacuoles formed in L3 connective cells; *stomium and CCC specification occur*	No vacuoles seen in pre-CCC cells; slight differential staining in paraplast sections	No vacuoles seen in pre-stomium cells; difficult to distinguish from other L1 cells; slight differential staining of pre-stomium cells in paraplast sections
	−3	Meiosis begins; callose deposition between MMCells; *stomium and CCC specification occur*	Identify CCC cells by morphology; dense cytoplasm with few small vesicles, no large vacuoles as present in L2 and L3 neighbors; initial divisions occur; CCC is 2 cells deep in transverse section	Identify stomium cells by morphology; dense cytoplasm and absence of the large vacuole present in neighboring epidermal cells
	−2	Meiosis in progress; tapetum large and multinucleate;*CCC differentiation begins;* thick callose walls between MMCells	Distinct differential staining in paraplast sections; continued cell divisions with various angles of division planes; multiple small vesicles	Distinct differential staining in paraplast sections; single epidermal layer; small vesicles in stomium cells
	−1	Meiosis in progress; *CCC differentiation and division occur*	Similar to stage −2	Similar to stage −2
Phase 2	+1	Meiosis complete; microspores in tetrads; *CCC differentiation complete*; *stomium differentiation begins*; all sporophytic tissue formed	12–14 cells in a circular cluster 2–4 cells deep; cells expanding; small vesicles begin to aggregate	Cytoplasmically dense cells; vesicles present, but no vacuole; large nuclear to cytoplasmic ratio; a single layer within the epidermis
	+2	Microspores separate. *CCC degeneration begins; stomium differentiation and division occur*	Cells have expanded; vesicles aggregate to create large vacuole; deposition of calcium oxalate crystals; initiation of cell degeneration	Cell divisions initiated; periclinal cell division creates 2-cell structure across epidermis; vesicles aggregate to form large vacuole; cells remain small
	+3	Tapetum shrinks; *fibrous lignin bands appear in expanded endothecium and middle wall layers*; *stomium division occurs*; pollen grains begin to differentiate	Advanced cell degeneration; no cell contents other than calcium crystals; cell walls degenerate	Periclinal cell division generates a stomium three cells deep within the width of an epidermal cell; occasional anticlinal division generates a stomium 4 cells across
	+4	*CCC adjacent to stomium degenerated*; tapetum degenerates; *stomium differentiation complete*	Space previously occupied by circular cell cluster now only contains calcium crystals; no cellular features or cell walls	Stomium differentiation complete; multi-tiered structure with 9–12 cells that is 3 cells deep
	+5 to +11	*Fibrous bands intensify in endothecium and middle layer; connective degeneration occurs*; *anther becomes bilocular*; pollen grains form	CCC no longer present and a "hole" is left in its place within the anther	No major changes observed
	+12	*Stomium degenerates and breaks; walls flip open, pollen released and dehiscence occurs*		Stomium cell degeneration
	+13	Senescence		

[a]In solanaceous plants, CCC also known as intersporangial septum (e.g., tomato, Bonner and Dickinson 1989), hypodermal stomium (e.g., sweet pepper; Horner and Wagner 1992), or oxalate package (D'Arcy et al. 1996)

cluster, and stomium lead to pollen release at flower opening (Fig. 1, stages +9 and +12; Goldberg et al. 1993, 1995; Beals and Goldberg 1997). We showed previously that the tobacco *TA56 thiol endopeptidase* gene is a marker for cell degeneration events that occur within the connective, circular cell cluster, and stomium (Koltunow et al. 1990; Goldberg et al. 1995; Beals and Goldberg 1997). The mechanisms responsible for switching the anther from a cell differentiation program (phase 1) to a cell degeneration and death program (phase 2) are not known.

Previous studies in our laboratory with transgenic tobacco plants showed that a functional stomium is required for anther dehiscence (Beals and Goldberg 1997). Targeted ablation of either the circular cell cluster and stomium or the stomium alone using a cytotoxic *barnase* gene driven by cell-specific promoters generates anthers that do not dehisce (Beals and Goldberg 1997). This indicates that dehiscence is not simply a mechanical process, but involves specific, exquisitely timed, cellular events. In addition, we (Sanders et al. 1999) and others (Dawson et al. 1993, 1999; Park et al. 1996) identified a large number of *A. thaliana* male-sterile dehiscence mutants, including those that either fail to dehisce (Dawson et al. 1993, 1999; Sanders et al. 1999; Steiner-Lange et al. 2003) or are defective in the timing of anther dehiscence (Sanders et al. 1999, 2000; Stintzi and Browse 2000; Ishiguro et al. 2001; Park et al. 2002; Von Malek et al. 2002). Analogous mutants have been found in other plant species (Kaul 1988). One *A. thaliana* non-dehiscence mutant, *ms35*, has a defect in the *MYB26* transcription factor gene and lacks endothecial cell fibrous bands, indicating the importance of these cells in anther dehiscence (Dawson et al. 1999; Steiner-Lange et al. 2003). In contrast, several late-dehiscence *A. thaliana* mutants, such as *DELAYED DEHISCENCE1* (*DDE1*)/*OPR3* (Sanders et al. 2000; Stintzi and Browse 2000), *DELAYED DEHISCENCE2* (*DDE2*)/*ALLENE OXIDASE SYNTHASE* (Sanders et al. 1999; Park et al. 2002; Von Malek et al. 2002), and *DEFECTIVE IN ANTHER DEHISCENCE1* (*DAD1*) (Ishiguro et al. 2001), have defects in jasmonic acid (JA) biosynthesis, indicating that this hormone is involved in coordinating the timing of stomium breakage with flower development and opening. Other hormones, such as ethylene, auxin, and gibberellic acid (GA), play a role in dehiscence, because dehiscence mutant phenocopies can be induced by either blocking or over-expressing genes involved in hormone activity (Murray et al. 2003; Rieu et al. 2003; Cecchetti et al. 2004; Achard et al. 2004). The differentiation of specialized cell types required for anther dehiscence and the cell-degeneration processes that ultimately lead to pollen release at flower opening suggest that unique gene sets are required to program these events during anther development. What these genes are and how they are regulated remain to be determined.

The stomium and circular cell cluster provide a novel system to study the differentiation and cell-death processes that are required for anther dehiscence. As a first step, we investigated the cellular and morphological events that occur in these cells throughout tobacco anther development at the level of the transmission electron microscope (TEM). We addressed three main questions: (1) when do cells that give rise to the circular cell cluster and stomium become specified within the anther primordium? (2) what primordium cell layer differentiates into the circular cell cluster? and (3) how are events leading to circular cell cluster and stomium formation and degeneration coordinated? We found that (1) differentiation events leading to circular cell cluster and stomium formation within the notch region occur after locule development begins, (2) the circular cell cluster is derived from founder cells in the primordium L2 layer that are contiguous to L1 cells destined to become the stomium, (3) circular cell cluster differentiation and degeneration occur before analogous events in the stomium take place, and (4) plasmodesmata connections occur between cells of the stomium and circular cell cluster. In addition, we demonstrate that laser capture microdissection (LCM) can be used to isolate stomium cells from differentiating anthers, and to detect individual stomium mRNAs. We propose that cell signaling plays a major role in specifying the circular cell cluster and stomium within the notch region during anther development.

Materials and methods

Growth of plants

Tobacco plants (*Nicotiana tabacum* cv. Samsun) were grown in the greenhouse under natural light conditions (Goldberg et al. 1978). Floral stages (phase 1, stages −7 to −1; phase 2, stages +1 to +12) used to follow anther development were described by Koltunow et al. (1990).

Light microscopy of anther sections

Anthers were dissected from staged floral buds and fixed in glutaraldehyde as described by Cox and Goldberg (1988). The fixed anthers were dehydrated, embedded in paraffin, and sliced into 10 μm sections (Cox and Goldberg 1988). Sections were stained with 0.05% toluidine blue and photographed with Kodak Gold 100 film (ISO 100/21) using bright-field microscopy in an Olympus compound microscope (Model BH2, Olympus, Lake Success, N.Y.).

Transmission electron microscopy of anther sections

Staged anthers were hand-dissected and transverse sections (~1.0 mm) were fixed (2.0% glutaraldehyde, 0.05 M sodium phosphate pH 7.2, 0.1% tannic acid) for 2 h at room temperature, and then rinsed four times in 0.05 M sodium phosphate pH 7.2 (each rinse 15 min).

The anther sections were treated with 1% osmium tetroxide (in 0.05 M sodium phosphate pH 7.2) for 2 h at room temperature followed by dehydration in a graded ethanol series (10%, 20%, 35%, 50%, 70%, 85%, 95%, each for 30 min and three times in 100% ethanol, each for 1 h). The addition of 0.1% tannic acid in the fixative was taken from Botha et al. (1993) to enhance preservation of membranes and plasmodesmata structures. The anther sections were embedded in Spurr's epoxy resin (Spurr 1969; Ted Pella, Redding, Calif.) and sectioned using an ultramicrotome (Sorvall Model MT-600, Dupont, Wilmington, Del.). Sections of 1 μm (stained with 1.0% toluidine blue at 42°C for 1–2 h) were examined to determine the region of the anther for further analysis and then 80 nm ultra-thin sections were prepared for TEM. These sections were placed on formavar-coated grids and stained with uranyl acetate and lead citrate. The anther sections were observed in a JEOL electron microscope 100CX II (JEOL, Peabody, Mass.) at 80 kV.

Transmission electron micrographs and figure preparation

The electron micrographs of anther notch regions and plasmodesmata were taken with Kodak EM film no. 4489. The electron micrographs of the tobacco anther notch were taken at a magnification of 1,900×. At later stages of development, several individual electron micrographs were required to encompass the area of interest. For example, at anther stage −5, the composite photograph of the notch region was comprised of six negatives, whereas at anther stage +4 the composite notch region photograph was comprised of 32 negatives. Individual photographs were joined together to create a composite image that was then digitally scanned (600 dpi) into a computer, either from the original image or from a copy negative for large format originals. The images were manipulated digitally with Adobe Photoshop (Adobe Systems, San Jose, Calif.) to enhance contrast and to remove the outlines of individual photographs. The electron micrographs of plasmodesmata were taken at a magnification of 29,000×. The plasmodesmata images presented in Figure 8 were digital scans (600 dpi) of the TEM micrographs that were captured at 300% of their original size.

LCM of stomium cells

Stage +6 anthers were trimmed to ~4 mm and processed for LCM according to Kerk et al. (2003), using ethanol:acetic acid fixative. Fixed anthers were embedded in paraffin (Paraplast-plus, Fisher Scientific, Pittsburgh, Pa.) according to procedures used for in situ hybridization experiments in our laboratory (Cox and Goldberg 1988). Anthers were sliced into 10 μm transverse sections (Reichert Jung 820-II Histocut Rotary Microtome), floated in water onto penfoil slides (Leica Microsystems, Bannockburn, Ill.), dried overnight at 42°C on a slide warmer (Fisher Scientific), and stored at room temperature until used. Prior to LCM, anther sections were de-paraffinized in xylene (two changes of 2 min each) and air-dried for 1 h. Approximately 45 stomium regions (400–500 cells) were captured from unstained anther sections using a Leica AS LMD Microdissection System (Leica Microsystems).

Real-time quantitative reverse transcription-polymerase chain reaction

LCM-captured stomium RNA was isolated using a PicoPure RNA Isolation Kit (Arcturus, Mountain View, Calif.), treated with RNase-free DNase I (Ambion, Austin, Tex.), purified using RNeasy Plant Mini Kit (Qiagen, Valencia, Calif.), and eluted into 15 μl RNase-free water. Complementary DNA (cDNA) was synthesized in a 20 μl reaction with an iScript cDNA Synthesis Kit (Bio-Rad, Hercules, Calif.), using all of the stomium RNA as a template. One-fortieth of the cDNA volume (0.5 μl) was amplified by quantitative polymerase chain reaction (qPCR) in a 25 μl reaction volume using iQ SYBR Green Supermix and an iCycler iQ Real-Time PCR Detection System (Bio-Rad). The following primers were used: TA56 Fw 5′-gctttggtacttaggcttggtgagagt-3′; TA56 Rv 5′-cttggtctttgacaggagtaacagcac-3′; TA20 Fw 5′-ctgccatgaaattgaatcctacaaatg-3′ TA20 Rv 5′-cgaaggtaagtagaaaggatggaggtg-3′ (Koltunow et al. 1990; Beals and Goldberg 1997).

Results

Locule differentiation occurs prior to the visible appearance of the circular cell cluster and stomium in the notch region

We studied the development of cells within the anther notch using TEM. We focused on circular cell cluster and stomium development to characterize their individual roles in establishing the site of wall breakage in anther dehiscence. Our studies were carried out at a low TEM magnification (1,900×), which afforded a greater resolution of the cells and cellular events than could be observed in either Paraplast or plastic sections with the light microscope. Using TEM, we characterized events in the anther notch from stages −7 to +5 and +9 to +12 of anther development (Fig. 1; Tables 1, 2). Our goal was to visualize events that (1) generate the differentiated circular cell cluster and stomium, and (2) create the site for dehiscence along the anther wall.

Figure 2 shows the initial changes that occurred within the stamen primordium to generate a four-locule anther. In transverse section, the primordium was a uniform collection of cells (Fig. 2, stage −7). By stage −6, cell divisions changed the round primordium into an

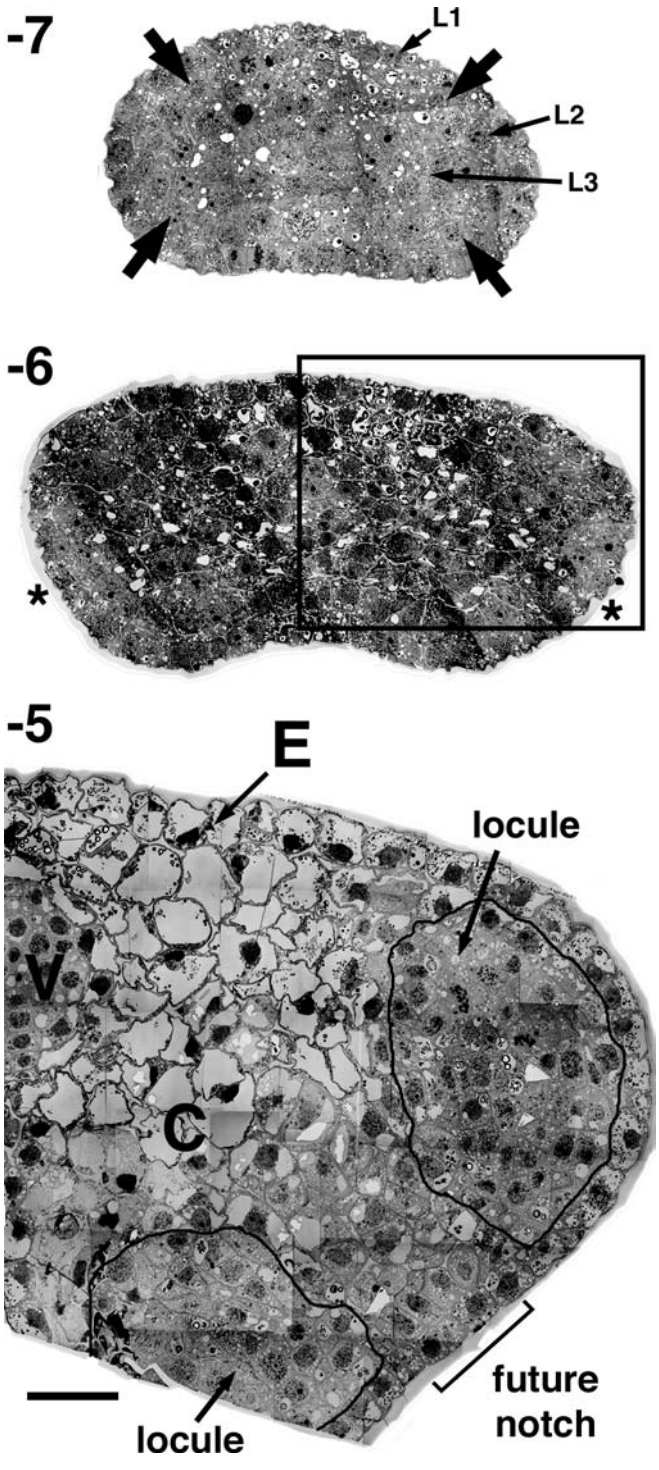

Fig. 2 Establishment of anther shape from the stamen primordia. Anther sections from stages −7, −6, and −5 were fixed, embedded in Spurr's epoxy resin, sliced into ultra-thin sections and prepared for transmission electron microscopy (TEM) as described in Materials and methods. TEM micrographs were taken at a magnification of 1,900×. The images of stages −7 and −6 are complete transverse sections of stamen primordia. The *boxed* area in stage −6 represents the region of the developing anther shown for stage −5. Stage −7, complete transverse section of a stamen primordium; *arrows* sites of archesporial cell differentiation, whose cell lineages will generate the four reproductive locules. Stage −6, complete transverse section of a stamen primordia; *asterisks* site of future anther notch regions, one of which is shown in the stage −5 partial transverse section. Stage −5, partial transverse section of a developing anther; *cells outlined in black* regions of developing locules. The designation of cells contained within the black border is based on their histology. These cells show mitotic activity and have not yet expanded or acquired large vacuoles. In a stage −5 anther, the cell-types contained within the L2-derived anther locules are the endothecium, middle layers, tapetum and sporogenous cells. The future notch is indicated between the two developing anther locules. *C* Connective; *E* epidermis; *Locule* region derived from the L2-archesporial lineage that will create the anther locule; *L1*, *L2, L3* the three cell layers present within the stamen primordia; *V* vascular region. *Bar* 30 μm

elongated structure (Fig. 2). At stages −7 and −6, the cells of the anther were relatively small in size and highly cytoplasmic with prominent nuclei. The stereotyped four-locule pattern of the anther began to emerge after stage −6 (Fig. 2, stage −6). At stage −5, the differentiation events within the future locule territories were apparent (Fig. 2, stage −5). Mitotic activity was observed in the four corners of the developing anther (Fig. 2, stage −5). In addition, cells of the developing connective and central region of the anther had acquired large vacuoles and expanded in size. Cells destined to become the vascular bundle could be identified and were round in shape and cytoplasmically dense with prominent nuclei (Fig. 2, stage −5). In contrast, we did not observe any distinctive cell types or mitotic activity in the region between the developing microsporangia (Fig. 2, stages −7 to −5). Epidermal and sub-epidermal cells in this region were indistinguishable from their adjacent neighbors (Fig. 2, stages −7 to −5), i.e., cells destined to become the circular cell cluster and stomium were not yet apparent within L1, L2, or L3 cell layers of the pre-notch region. Together, these results indicate that the initial developmental events in the anther primordium, including the differentiation of cells that generate the locules, occur prior to any visible cellular events within the site of the future anther notch (Figs. 1; 2; Table 1).

The circular cell cluster is derived from cells of the primordium L2 layer

We examined both bright-field photographs and TEM micrographs of sections throughout phase 1 of anther development to determine when the circular cell cluster and stomium cells became specified within the notch region (Table 1). Figure 3 shows the developing notch region from stages −5 to −1. We aligned these photographs so that (1) cells within the developing notch are in the center, and (2) the same area of each anther is shown in both the bright-field photographs (Fig. 3A–E) and TEM micrographs (Fig. 3F–H). Light microscopy allowed us to obtain an overview of notch-region development in parallel with other developmental events that occurred within the anther (e.g., locule formation).

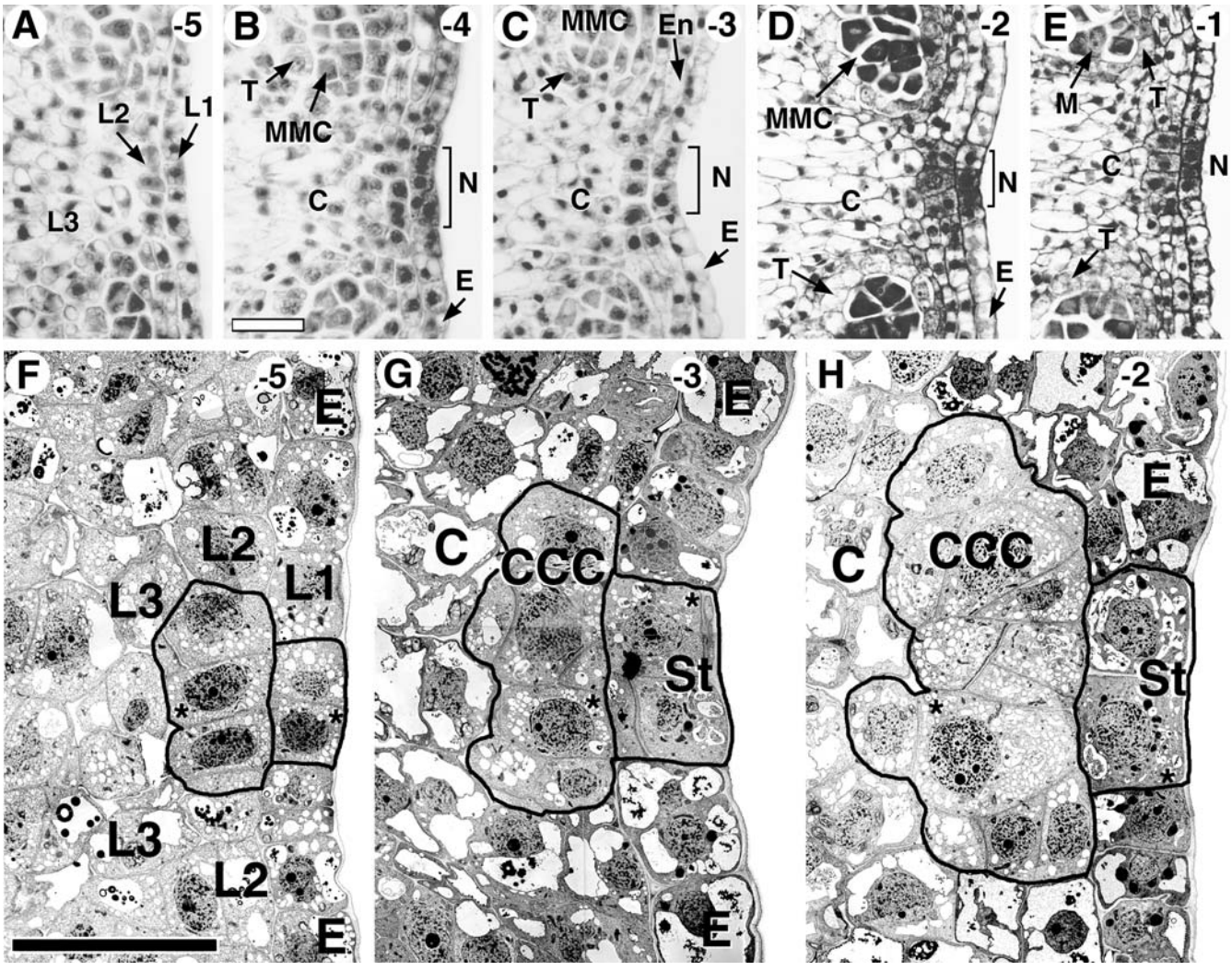

Fig. 3A–H Development of the anther notch at stages −5 to −1. Anthers were fixed and embedded in both paraffin and Spurr's epoxy resin as described in Materials and methods. Paraffin-embedded anthers were sliced into 10 μm transverse sections, stained with toluidine blue and the notch regions were photographed by bright-field microscopy. Spurr's embedded anthers were sliced into ultra-thin sections and prepared for TEM. Anther developmental stages are shown in the top right corner of each photograph. The stomium and the circular cell cluster span the length of the anther and are a long column of cells of which these photographs represent a single layer. In TEM micrographs, the cells of the stomium and the circular cell cluster are highlighted by a *black border*. **A–E** Bright-field photographs of the developing anther notch. **A** Stage −5, **B** stage −4, **C** stage −3, **D** stage −2, **E** stage −1. **F–H** TEM micrographs of the developing anther notch. **F** Stage −5, **G** stage −3, **H** stage −2. The stage −5 notch is a consecutive section from the anther shown in Fig. 2. The circular cell cluster and stomium cells marked with an *asterisk* are shown in greater detail in Figs. 4 and 7. *C* Connective; *CCC* circular cell cluster; *E* epidermis; *En* endothecium; *L1*, *L2, L3* the three cell layers present within the stamen primordia; *M* meiocyte; *MMC* microspore mother cells; *N* notch; *St* stomium; *T* tapetum. *Bars* **B** 20 μm (also the scale for **A**, **C**, **D**, **E**), **F** 30 μm (scale for **G**, **H**)

In contrast, TEM enabled us to obtain a detailed characterization of the developing notch region at the cellular level. We were able to determine which cells within the notch became the circular cell cluster and stomium by visualizing events within specific cell layers at later stages (e.g., stages −3 to −2) and then tracing the cell lineages backwards to earlier stages (e.g., stage −5).

At the level of the light microscope, circular cell cluster and stomium cells within the pre-notch region could not be distinguished at stages −5 to −3 (Fig. 3A–C). In contrast, cells within developing locule territories (e.g., microspore mother cells, tapetum) could be identified by their shape, differential staining, and mitotic activity (Fig. 3A–C). Epidermal and connective cells were also identified at this time of development (Fig. 3A–C). By stages −2 and −1, L1 and L2 cells within the interlocular region could be distinguished from their neighbors by differential staining (Fig. 3D–E; data not shown), suggesting that notch-region cells destined to become the circular cell cluster and stomium have been specified by this stage of anther development.

At the resolution of the TEM, changes within cells destined to become the circular cell cluster were detected earlier than with the light microscope. At stage −5, cells within the future notch region were relatively uniform and could be distinguished only by their location within

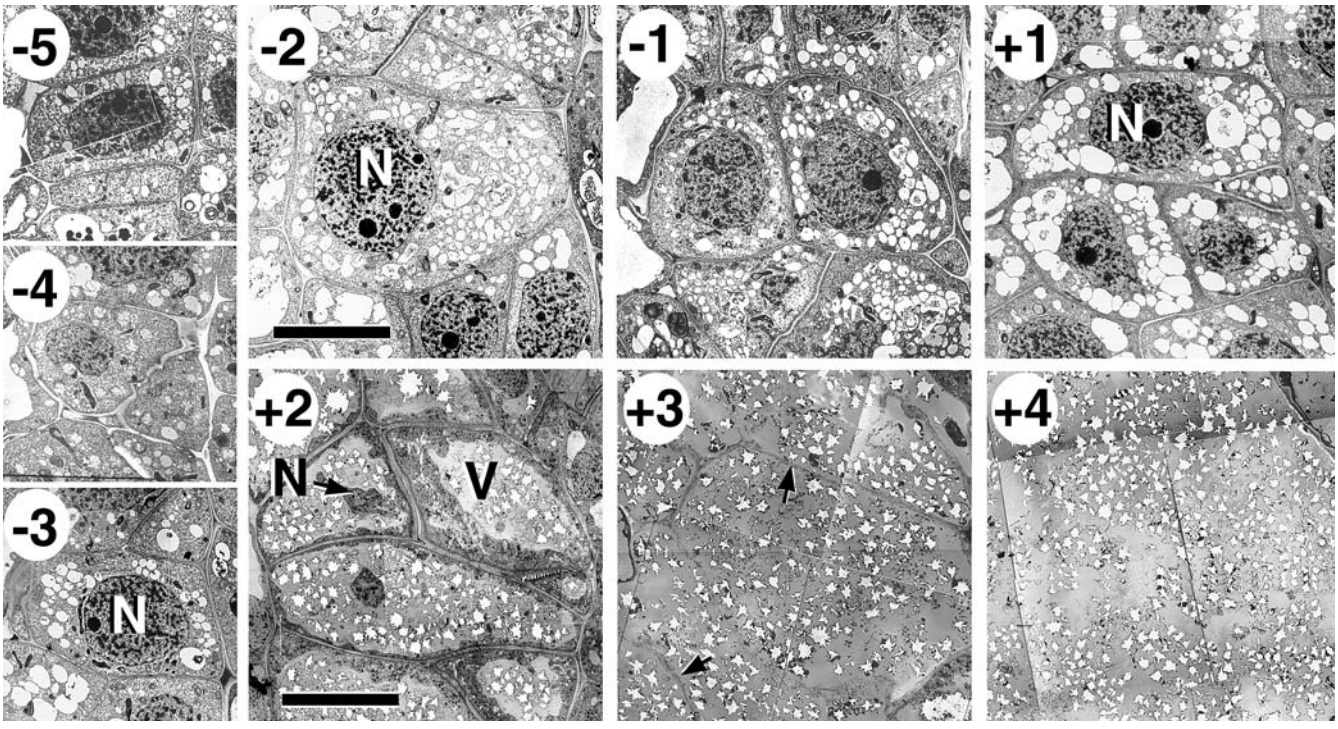

Fig. 4 Cells of the circular cell cluster during tobacco anther development. Stage −5 to +4 anther sections were fixed, embedded in Spurr's epoxy resin, sliced into ultra-thin sections and prepared for TEM as described in Materials and methods. The images presented here are close-ups of the circular cell cluster cells marked with an *asterisk* in Figs. 3 and 6. The nuclei at stage +2 are distorted and shrunken. The white star-like shapes at stages +2 to +4 represent calcium oxalate druse crystals. The *arrows* in stage +3 indicate cell wall remnants of the degenerating circular cell cluster. *N* Nucleus, *V* vacuole. *Bars* Stage −2 10 μm (scale for stages −5 to +1), stage +2 20 μm (scale for stages +2 to +4)

the primordium L1, L2, and L3 layers (Figs. 2, stage −5; 3F). The L1 and L2 cells within the future notch region were relatively uniform in appearance, cytoplasmically rich, and contained small vesicles and/or vacuoles (Fig. 3F). In contrast, L2 cells outside of the pre-notch region in the corners of the primordium had divided to generate the developing locules (Figs. 2, stage −5; 3A). In addition, L3 cells flanking the future notch region were more vacuolate in appearance than neighboring L2 and L1 cells (Figs. 2, stage −5; 3F). This also was the case for epidermal cells contiguous to the L1 cells of the future notch site (Figs. 2, stage −5; 3F). Within the notch, pre-circular cell cluster and stomium cells were visualized as a single layer of L2 and L1 cells, respectively (Fig. 3F).

By stages −3 and −2, the circular cell cluster was identified as a group of distinctively-shaped L2-derived cells between the L1 epidermis and the L3-derived connective layers (Fig. 3G, H). Cells within the L2 layer destined to become the circular cell cluster divided, expanded, and accumulated numerous small vesicles (Fig. 3F–H). In contrast, L1 epidermal cells that bordered the developing circular cell cluster (i.e., pre-stomium cells) did not divide and remained cytoplasmically dense (Fig. 3F–H). Cells surrounding the pre-notch region accumulated large vacuoles and were visibly distinct compared with pre-circular cell cluster and pre-stomium cells (Figs. 2, stage −5; 3G, H). By stage −2, the TEM micrographs showed that the circular cell cluster formed a group of histologically distinct cells within the developing anther notch (Fig. 3H)—the same stage as when differential staining was observed within this area in the Paraplast sections (Fig. 3D).

Figure 4 shows TEM close-ups of individual circular cell cluster cells at different stages of anther development. During stages −5 to −2, cells of the circular cell cluster increased significantly in size and accumulated numerous small vesicles (Fig. 4; Table 1). Figure 5A shows that a large increase in the number of cells contained within the circular cell cluster occurred during stages −5 to −1. The number of cells within the circular cell cluster reached a maximum of ∼14 by stage −2 in a typical transverse 10 μm section (Fig. 5A–C). This increase was due primarily to periclinal cell divisions that increased the number of cell layers (Figs. 3; 5A–C). Together, these results show that the circular cell cluster is specified from L2 cells within the pre-notch region and that circular cell differentiation events can be visualized as early as stage −3, prior to any changes in contiguous pre-stomium cells in the L1 layer.

Circular cell cluster differentiation and degeneration occur before analogous stomium events take place

We studied the developing notch region from stages +1 to +4 in both the light microscope and TEM to characterize developmental changes within the circular cell

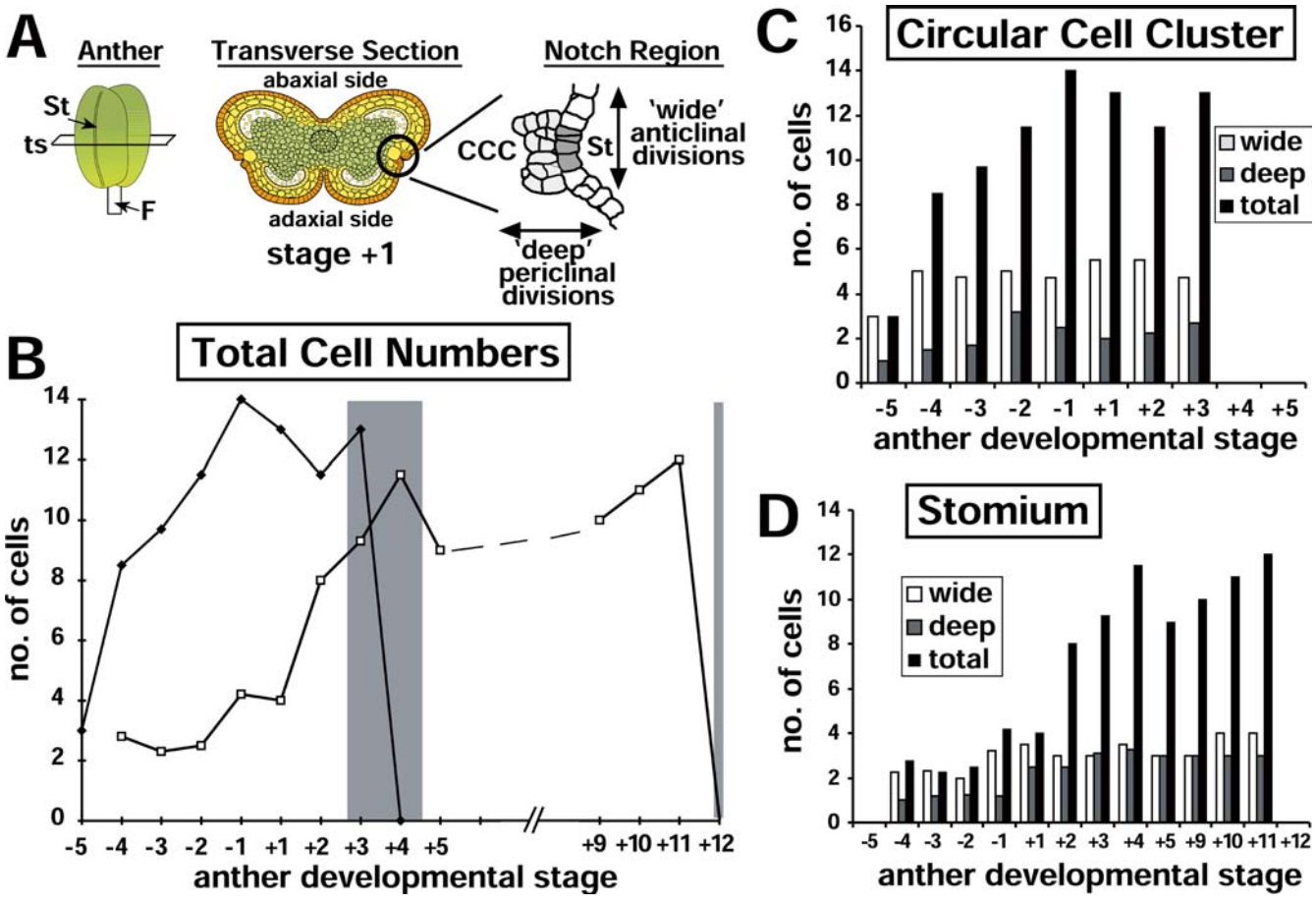

Fig. 5A–D Number of cells in the circular cell cluster and stomium during anther development. The number of cells in the circular cell cluster and stomium during anther development were counted from transverse sections visualized in the TEM (Figs. 3, 6, 9; data not shown). The total number of circular cell cluster and stomium cells in the entire anther is larger. Anther developmental stages are from Koltunow et al. (1990); phase 1, stages −7 to −1 and phase 2, stages +1 to +12). **A** Cartoon representation of sectioning used to view notch region cell types. Transverse sections through the anther generate a butterfly shape. TEM analysis focused on the notch region of each transverse section. Periclinal cell divisions generated an increase in the width (*deep*) of the circular cell cluster and stomium as observed in transverse section. Anticlinal cell divisions generated an increase across (*wide*; adaxial to abaxial) the circular cell cluster and stomium as visualized in transverse section. **B** Total number of cells in the circular cell cluster and stomium at different stages of anther development. *Closed diamonds* Circular cell cluster, *open squares* stomium. Cell numbers were not counted between stages +6 to +8 (*dashed line*). *Shaded areas* Periods of cell-death: stages +3 to +4 for the circular cell cluster and stage +12 for the stomium. Cells in one to four sections were counted depending upon the stage. **C** Number of circular cell cluster cells in transverse sections at different stages of anther development. **D** Number of stomium cells in transverse sections at different stages of anther development. *Bars* Average number of cells in counted transverse sections

cluster and to identify when stomium differentiation began (Figs. 4; 6; Table 1). The bright-field photographs presented in Figure 6A, B showed that by stages +1 and +2 the circular cell cluster had formed into the circular arrangement of sub-epidermal cells for which it was named (Koltunow et al. 1990); i.e., circular cell cluster differentiation had occurred. From stages +2 to +4 major changes were observed in the notch region at the level of the light microscope (Fig. 6B–D; Table 1). Circular cell cluster degeneration took place, the stomium differentiated from contiguous L1 layer cells, fibrous bands were deposited in the endothecium and middle layer, and the epidermal cells neighboring the developing stomium expanded and contained a single, large vacuole (Fig. 6B–D; Table 1; data not shown).

TEM micrographs of the developing notch region from stages +1 to +4 are shown in Figure 6E–H, and close-ups of individual circular cell cluster cells at these stages are shown in Figure 4. At stage +1, the cells of the circular cell cluster had a distinctive round shape and lacked the large vacuole seen in surrounding cells (Fig. 6A, E). The circular cell cluster was two to three cells deep (or across) in a typical section due to periclinal cell divisions (Figs. 5A; 6E). The small vesicles that accumulated during stages −5 to −2 (Figs. 3F–H; 4) had begun to aggregate (Figs. 4; 6E). By stage +2, the cells of the circular cell cluster underwent further expansion and contained a single large vacuole (Figs. 4; 6B,F). The circular cell cluster size increase was caused by cell enlargement and not by cell division, as the number of cells did not increase after stage −1 (Fig. 5B,C). The vacuole present in cells of the stage +2 circular cell cluster was formed by aggregation of small vesicles that

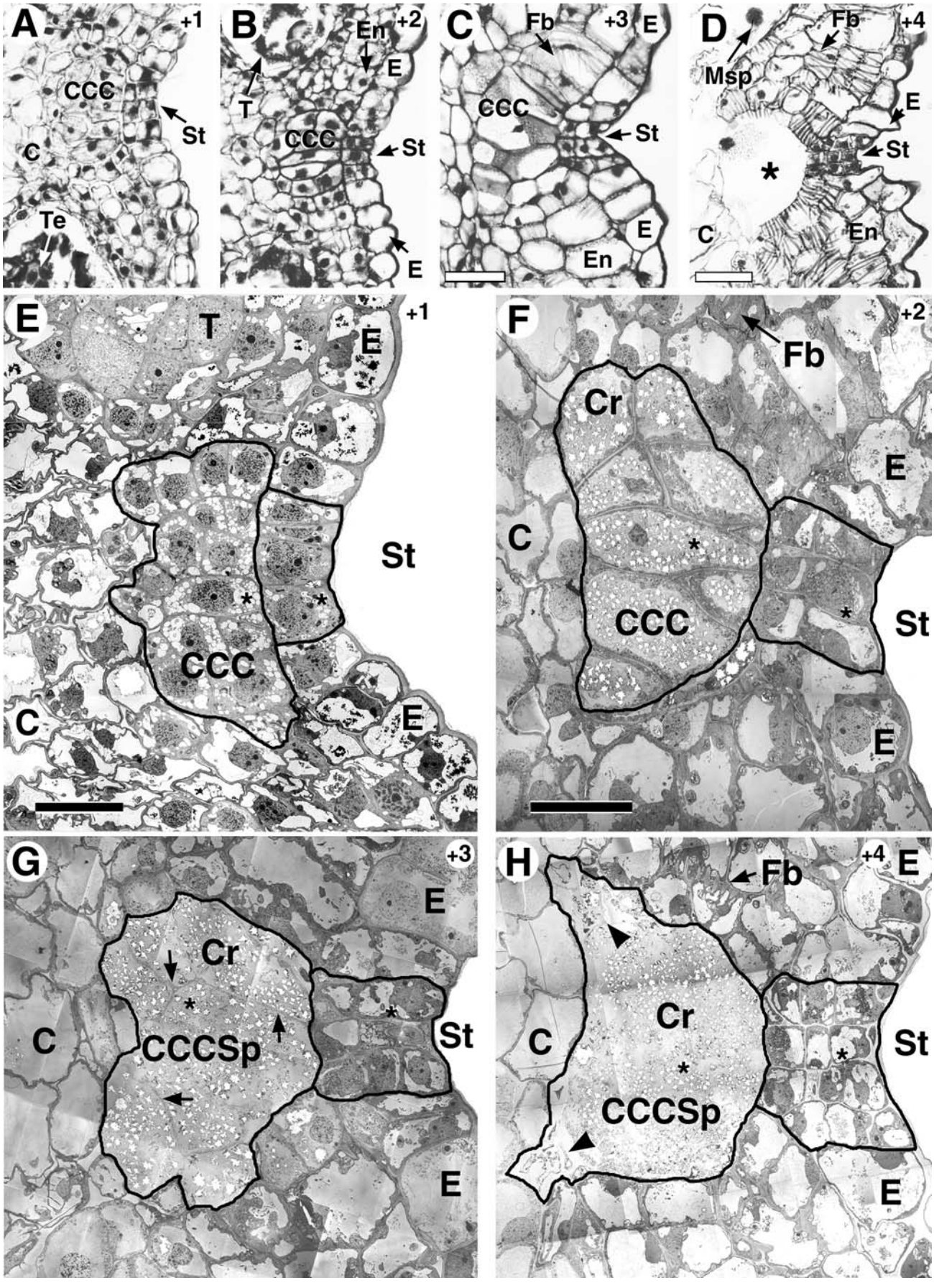
A
+1
CCC
St
C
Te
B
En
+2
E
T
CCC
St
E
C
+3
Fb
E
CCC
St
E
En
D
Fb
+4
Msp
E
St
*
C
En
E
T
E
+1
St
CCC
C
E
F
+2
Fb
Cr
E
C
*
CCC
St
E
G
+3
E
Cr
C
CCCSp
St
E
H
Fb
+4
E
Cr
C
CCCSp
St
E

◀

Fig. 6A–H Circular cell cluster degeneration and stomium differentiation. Anther sections from stages +1 to +4 were fixed and embedded in either Paraplast or Spurr's epoxy resin as described in Materials and methods. Paraffin-embedded anthers were sliced into 10 μm transverse sections, stained with toluidine blue, and notch regions were photographed by bright-field microscopy. Spurr's embedded anthers were sliced into ultra-thin sections and prepared for TEM. Anther developmental stages are shown in the top right corner of each photograph. In the TEM micrographs, the cells of the stomium and circular cell cluster are highlighted by a *black border*. **A–D** Bright-field photographs of the developing anther notch region. **A** Stage +1, **B** stage +2, **C** stage +3, **D** stage +4. In **D** the *asterisk* represents the space previously occupied by the circular cell cluster. **E–H** TEM micrographs of the developing anther notch region. **E** Stage +1, **F** stage +2, **G** stage +3, **H** stage +4. *Black borders* (**E–H**) surround the circular cell cluster and stomium. In **G**, *arrows* indicate cell wall remnants from circular cell cluster degeneration and in **H**, *arrowheads* indicate initial stages of connective cell degeneration. The *black border* in **H** surrounding the space left by the degenerated circular cell cluster includes neighboring connective cells that are degenerating (*arrowheads*). The circular cell cluster and stomium cells marked with an *asterisk* are shown in greater detail in Figs. 4 and 7. *C* Connective, *CCC* circular cell cluster, *CCCSp* space generated by degeneration of circular cell cluster cells, *Cr* calcium oxalate crystals, *E* epidermis, *En* endothecium, *Fb* fibrous bands, *Msp* microspore, *St* stomium, *T* tapetum, *Te* tetrad. *Bars* **C** 20 μm (scale for **A**, **B**), **D** 25 μm, **E** 30 μm (scale for **G**, **H**), **F** 30 μm

had accumulated earlier (Figs. 3; 4; 6E,F). The cytoplasm within these cells was compressed against the cell wall and the nucleus appeared shrunken and distorted (Figs. 4; 6F). In addition, calcium oxalate druse crystals (Horner and Wagner 1980; D'Arcy et al. 1996) were present within the large vacuoles of the stage +2 circular cell cluster and were visualized as "white-star" shapes in TEM micrographs (Figs. 4; 6F). The "white-stars" represented holes left behind after sectioning, as the crystals were not sectioned. The presence of calcium oxalate crystals contributed to the speckled appearance of the circular cell cluster cells in the light microscope (Fig. 6C).

The creation of a single large vacuole, the accumulation of calcium oxalate crystals, and the shrinking of the nucleus in cells of the circular cell cluster at stage +2 marked the beginning of the circular cell cluster degeneration program (Fig. 6C,D,F,H). By stage +3, all that remained of the circular cell cluster was vacuole contents and cell wall remnants (Figs. 4; 6G). The druse crystals and the vacuole contents in which they were embedded remained in the space occupied previously by the circular cell cluster (Figs. 4; 6G–H). By stage +4, the wall remnants were completely degenerated and cells of the circular cell cluster were no longer present, leaving a large circular hole in the anther (Figs. 4; 6D,H; Table 1).

Connective cells contiguous to the circular cell cluster and the tapetum also began to degenerate during this period (stages +2 to +4) resulting in a bilocular anther (Figs. 1; 6D,F,H; Table 1). In addition, the notch region became more pronounced as a consequence of locule territory enlargement, the endothecium expanded, and lignified fibrous bands (Manning 1996) were deposited within both connective and endothecial cells (Fig. 6C,D,F,H; Table 1). Together, these results show that circular cell cluster differentiation occurred between stages −3 and +1 of anther development and that cells of the circular cell cluster underwent a programmed cell death process and degenerated by stage +4 (Fig. 6D,H; Table 1).

Stomium cells are specified early in the development of the notch region

When do the L1 cells within the anther primordium give rise to the stomium and how do events that occur within the stomium compare with those observed in the circular cell cluster during anther development? At stage −5, L1-layer primordium cells in the future notch region were indistinguishable from each other in both the light microscope (Fig. 3A) and the TEM (Figs. 2 stage −5; 3F). These included the L1 cells immediately adjacent to L2 cells that gave rise to the circular cell cluster and their L1 neighbors (Fig. 3A,F). At stage −3, in contrast, L1 cells destined to become the stomium were cytoplasmically dense and did not contain large vacuoles like their neighboring L1 epidermal cells (Fig. 3C,G). Typically, two or three pre-stomium L1 cells were observed in TEM transverse sections at stages −3 and −2, and these cells were in contact with the differentiating circular cell cluster (Figs. 3G,H; 5D). At the light microscope level, L1-layer pre-stomium cells stained more intensely with toluidine blue than did their epidermal neighbors at stages −2 and −1, similar to those in the developing circular cell cluster (Fig. 3D,E; data not shown). Together, these data show that a small number of L1-layer primordium cells become specified as early as stage −3 to follow a stomium differentiation pathway, and that these cells can be distinguished from neighboring epidermal cells by their staining properties, dense cytoplasm, absence of prominent vacuoles, and contact with the differentiating circular cell cluster.

Development of a multi-layered stomium occurs after the circular cell cluster degenerates

The pre-stomium cells within the L1 layer did not undergo any detectable changes during stages −3 to −1 of anther development at the level of either the light or electron microscope (Figs. 3; 7). Close-ups of individual pre-stomium cells indicate that they had a high nuclear to cytoplasmic volume and only small vesicles or vacuoles (Fig. 7). Nor did they increase significantly in number during this period, in contrast with cells of the circular cell cluster (Fig. 5B,D).

From stages +1 to +4, however, the pre-stomium cells underwent several divisions, including two periclinal divisions and an occasional anticlinal division (Figs. 5B,D; 6E–H). At stage +2, one periclinal division generated a developing stomium that was three cells across and two cells deep in a typical section—approximately the width of a single epidermal cell (Figs. 5D;

6F). At stage +3, a second periclinal division generated a stomium that was three cells across and three cells deep (Figs. 5D; 6G). In some sections, we observed four rows of stomium cells, suggesting that an anticlinal cell division had occurred (Fig. 6E). Thus, by stage +4 the mature stomium was a group of approximately 9–12 small cells that were positioned within the epidermal layer of the anther (Figs. 5B,D; 6 C,D,G,H; Table 1). The multi-tiered stomium was clearly distinguished from contiguous epidermal cells that were larger and more highly vacuolate (Fig. 6 C,D,G,H). Individual stomium cells remained histologically similar during stages +3 to +5 (Figs. 6G,H; 7), but expanded and acquired prominent vacuoles, structures not apparent in earlier stages of stomium cell development (Fig. 7, stages −5 to −1). Stomium cell division events occurred after the circular cell cluster stopped dividing (Figs. 5B; 6; Table 1). By the time a multi-tiered stomium formed, the circular cell cluster had degenerated (Figs. 5B; 6C,D,G,H; Table 1). Together, development of the stomium and the death of the circular cell cluster by stage +4 established the future site for anther wall breakage at dehiscence.

Plasmodesmata connections occur between cells within the notch region

We examined the boundaries between cells of the developing notch region to determine whether there were plasmodesmata connections, and, if so, what cells were connected by these cytoplasmic channels. The presence of plasmodesmata might provide clues to possible interactions between notch-region cell types (Haywood et al. 2002). We focused our efforts on stages −4 to +2, when both the circular cell cluster and stomium became specified and differentiated (Figs. 3; 6). To identify plasmodesmata, we used a higher TEM magnification (~29,000×) than that used to visualize notch region development (1,900×; Figs. 2; 3; 4; 6; 7).

Plasmodesmata were observed within the notch region at all developmental stages examined (Fig. 8). Connections occurred between similar cell types (e.g., stomium-stomium; Fig. 8, st-st) and different cell types (e.g., stomium-circular cell cluster; Fig. 8, st-ccc). Both

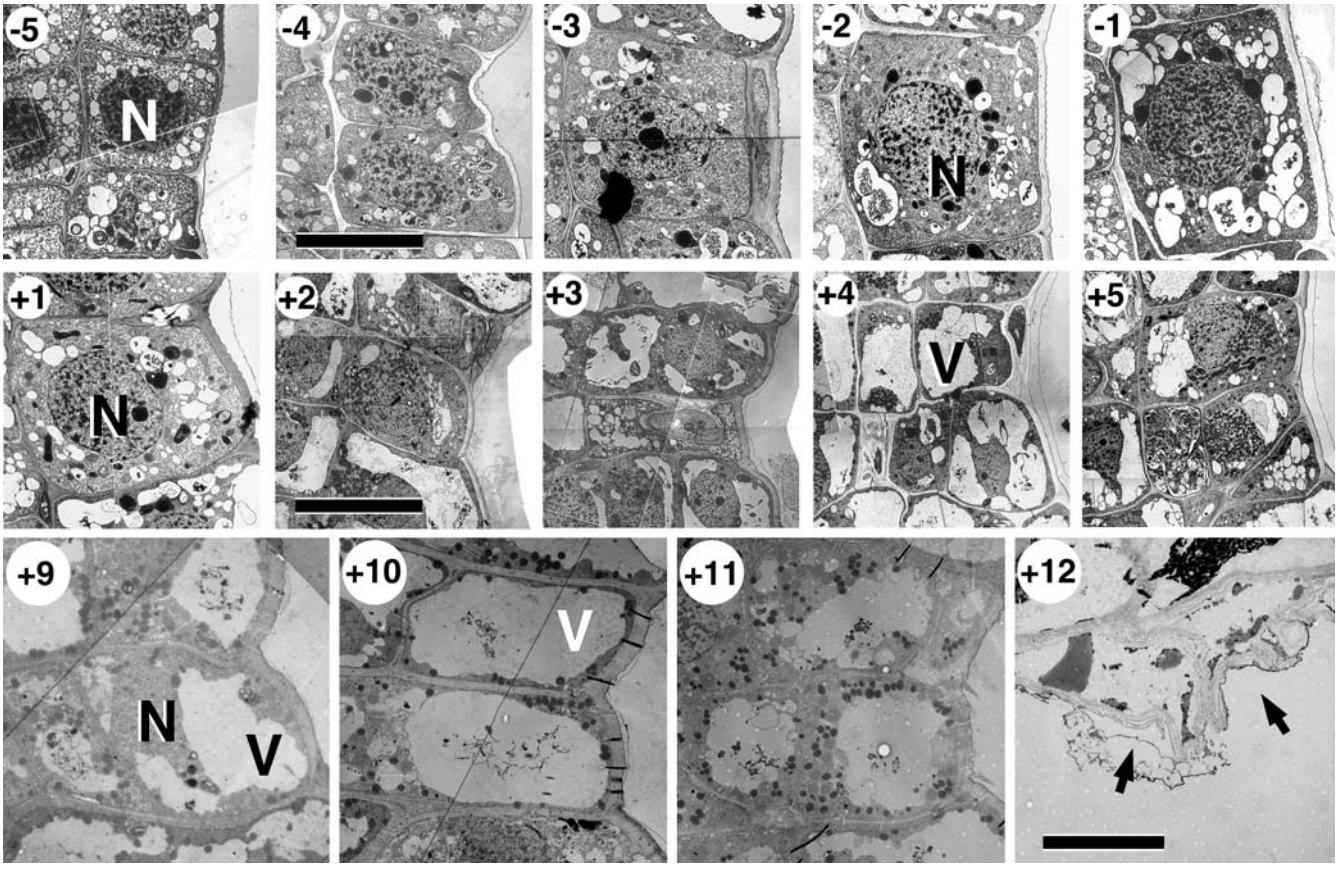

Fig. 7 Stomium cells during tobacco anther development. Anther sections from stages −5 to +5 and stages +9 to +12 were fixed, embedded in Spurr's epoxy resin, sliced into ultra-thin sections and prepared for the TEM as described in Materials and methods. The images presented here are close-ups of stomium cells marked with an *asterisk* in Figs. 3, 6, 9, and 10A. Stage +10 is from a consecutive transverse section from the same anther shown in Fig. 9. At stages +9 to +11, small dark lipid vesicles are seen to accumulate. The *black arrows* in stage +12 indicate the degenerated stomium cells after dehiscence and anther opening. *N* Nucleus, *V* vacuole. *Bars* Stage −4 10 μm (scale for stages −5 to +1), stage +2 20 μm (scale for stages +2 to +5), stage +12 10 μm (scale for stages +9 to +12)

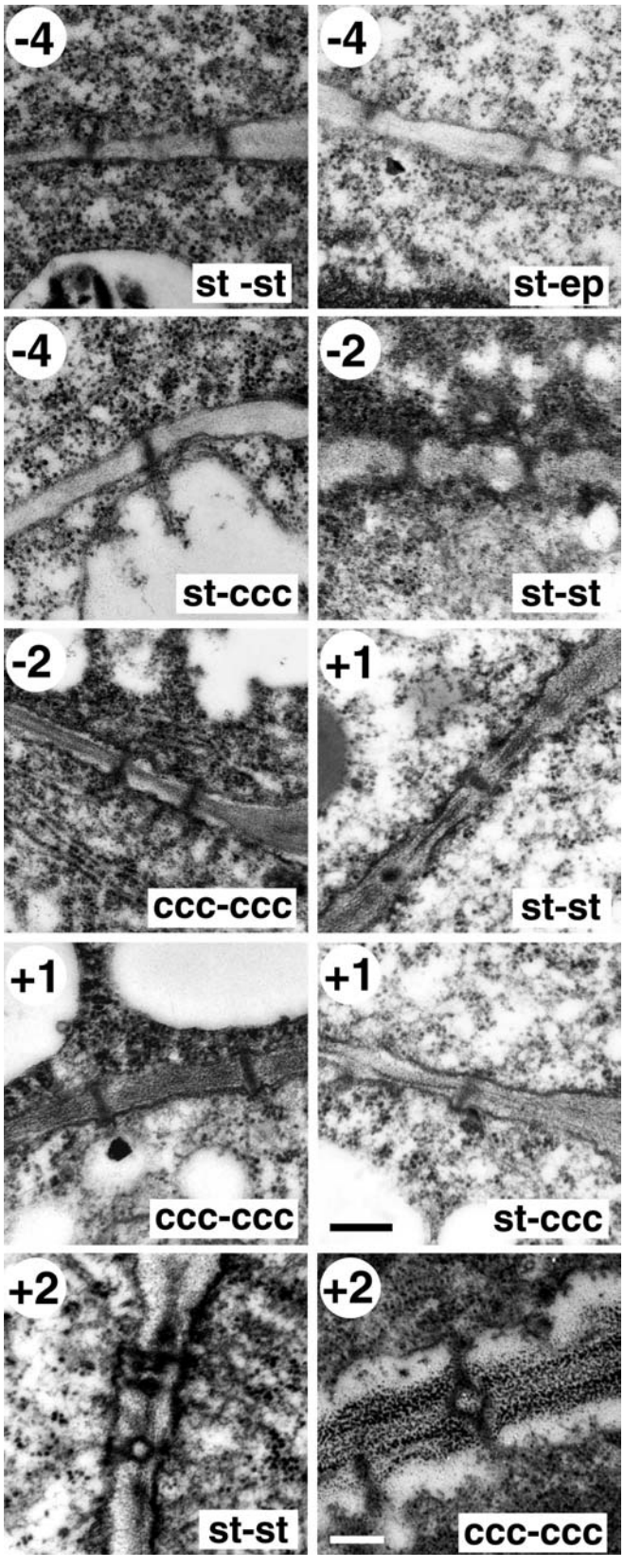

Fig. 8 Plasmodesmata in the anther notch region during anther development. Anther sections from stages −4, −2, +1, and +2 were fixed, embedded in Spurr's epoxy resin, sliced into ultra-thin sections and prepared for the TEM as described in Materials and methods. Primary plasmodesmata identified between the cells of the developing notch are shown for stages −4, −2 and +1. Secondary plasmodesmata are shown for stage +2. The labels refer to the borders between two cell-types: *st-st* between two stomium cells, *st-ep* between stomium and epidermal cells, *st-ccc* between stomium and circular cell cluster cells, *ccc-ccc* between two circular cell cluster cells. *Bars* Stage +1 200 nm (scale for stages −4 and −2), stage +2 200 nm

primary plasmodesmata (Fig. 8, stages −4 to +1) and secondary plasmodesmata (Fig. 8, stage +2) were detected. No differences were observed between the types of cells that were connected by plasmodesmata at different stages (data not shown). Nor were there detectable differences in the number of plasmodesmata connections observed between different cell types (data not shown). The only apparent change in plasmodesmata was visualized at the time of circular cell cluster degeneration—plasmodesmata connections between the circular cell cluster and other cell types disappeared (data not shown). Together, these results indicate that the entire notch region is connected by cytoplasmic channels and that plasmodesmata occur between the circular cell cluster and stomium when these cells become specified (Fig. 8, stage −4).

Stomium cell death establishes the site for pollen release at dehiscence

We examined the notch region at the terminal stages of anther development (stages +8 to +12; Table 1) in both the light microscope (Fig. 9A–D) and TEM (Figs. 9E–G; 10) to visualize cellular events that occurred within the stomium in the period prior to dehiscence (stages +8 to +11) and during dehiscence (stage +12). From stages +8 to +11 the stomium consisted of a multi-tiered set of cells flanked by calcium-oxalate-filled space left over from the degenerated circular cell cluster (Fig. 9A–G), similar to that observed earlier in anther development (Fig. 6H, stage +4). The stomium did not increase in cell number after stage +4 (Fig. 5B,D), and remained the narrowest site within the anther wall (Fig. 9A–C). Stomium cells were markedly smaller in size and contained prominent nuclei in comparison with neighboring epidermal and endothecial cells, which expanded significantly during this period and contained large vacuoles (Fig. 9A–G). In addition, fibrous bands became more numerous in both the endothecium and connective (Fig. 9A–D,F,H). The only visible change in the stomium cells from stages +9 to +11 was an increase in the number of lipid vesicles and an enlargement of vacuole size due to coalescence of smaller vacuoles (Figs. 7; 9E–G). During this period the stomium consisted of intact cells, i.e., stomium cell degeneration had not yet occurred.

We compared a mechanically-sheared stage +11 notch region (Fig. 10B) with one that dehisced at stage +12 (Figs. 7; 9H; 10A) to determine if stomium cell death played a role in the dehiscence process. Fixed, stage +11 anthers often break at the stomium when

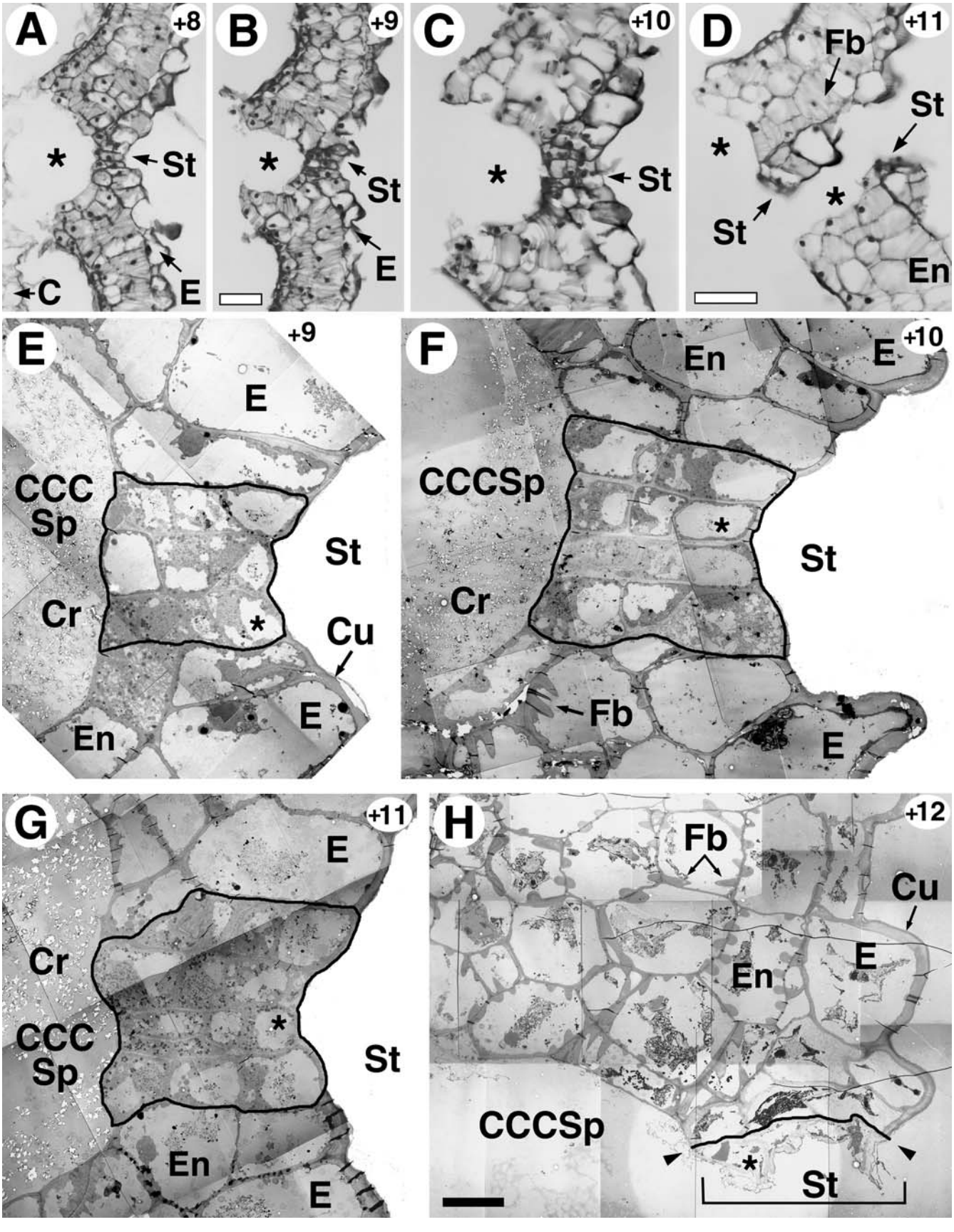
A
+8
St
C
E
B
+9
St
E
C
+10
St
D
+11
Fb
St
St
En
E
+9
E
CCC
Sp
St
Cr
Cu
E
En
F
+10
En
E
CCCSp
St
Cr
Fb
E
G
+11
E
Cr
CCC
Sp
St
En
E
H
+12
Fb
Cu
E
En
CCCSp
St

◀

Fig. 9A–H Late events in stomium development. Stage +8 to +12 anthers were fixed and embedded in either Paraplast or Spurr's epoxy resin as described in Materials and methods. Paraffin-embedded anthers were sliced into 10 μm transverse sections, stained with toluidine blue, and the notch regions were photographed by bright-field microscopy. Spurr's embedded anthers were sliced into ultra-thin sections and prepared for TEM. **A**–**D** Bright-field photographs of the developing anther notch. **A** stage +8, **B** stage +9, **C** stage +10, **D** stage +11. The *asterisks* in **A**–**D** represent the space previously occupied by circular cell cluster cells (see Fig. 6). The break at the stomium in the stage +11 anther in **D** was caused by mechanical shearing during sectioning, but demonstrates the biological process seen at anther dehiscence, stage +12. The space occupied previously by the circular cell cluster in **D** divided into two regions during sectioning and is marked by the *asterisks*. **E**–**H** TEM micrographs of the developing anther notch. **E** Stage +9, **F** stage +10, **G** stage +11, **H** stage +12. In **E**–**H** the stomium cells marked with an *asterisk* are shown in greater detail in Fig. 7. The *black border* in **E**–**G** outlines the stomium cells. The *black border* and *arrowheads* in **H** delineate the stomium from neighboring cells in the Stage +12 dehisced anther. *C* Connective, *CCCSp* space created by degeneration of the circular cell cluster, *Cr* calcium oxalate crystals, *Cu* cuticle, *E* epidermis, *En* endothecium, *Fb* fibrous bands, *St* stomium. *Bars* **B** 25 μm (scale for **A**), **D** 25 μm (scale for **C**), **H** 15 μm (scale for **E**, **F**, **G**)

sectioned, as illustrated by the bright-field section shown in Figure 9D. The weakness of the stage +11 stomium probably reflects cellular changes (e.g., degeneration events) that occur in preparation for dehiscence at stage +12 (Figs. 1; 10). The TEM analysis of a sheared stage +11 stomium showed that both sides of the anther wall were in close proximity to each other and that the cells were intact (Fig. 10B). In addition, calcium oxalate crystals were still present in the torn stage +11 notch region (Fig. 10B). This was in marked contrast to the stomium at dehiscence (Figs. 9H; 10A). Figure 10A shows a dehisced stage +12 anther with both sides of the wall positioned across the breakage point, the top half of which is shown in Figure 9H. All cells within the dehisced notch region (e.g., connective, endothecium) showed that the initial stages of senescence had begun—cells were distorted and their cytoplasmic contents had pulled-away from cell membranes and walls (Figs. 9H; 10A). In addition, the calcium oxalate crystals had disappeared (compare Figs. 9H and 10A with Fig. 9E–G). In contrast with intact epidermal and endothecial cells at stage +12, the stomium appeared to have crumpled, collapsed, and degenerated (Figs. 7; 9H; 10A). Together, these results show that stomium cells remained intact within the anther wall up to stage +11, and that they underwent a cell-death program at stage +12 similar to one that occurred earlier within the circular cell cluster (Fig. 6E–H). Stomium degeneration allowed the anther wall to break and release pollen at flower opening (Fig. 1).

LCM can be used to detect specific stomium mRNAs

We used LCM to determine whether we could isolate stomium cells and detect the presence of specific stomium mRNAs (Kerk et al. 2003). LCM is a powerful tool for using genomic approaches (Asano et al. 2002; Kerk et al. 2003; Nakazano et al. 2003) to identify the genes and proteins that function within the circular cell cluster and stomium during anther development and that are critical for the dehiscence process. Figure 11 shows a transverse section of a stage +6 anther notch region before LCM (Fig. 11A) and after LCM (Fig. 11B). We were able to capture the entire cluster of stomium cells from the notch region and separate it from the rest of the anther using LCM (Fig. 11B).

We isolated RNA from 45 captured stomium cell clusters containing a total of approximately 450 cells (Fig. 5D), and used real-time quantitative reverse transcription-PCR (qRT-PCR) to detect the presence of TA56 and TA20 mRNAs that we had shown previously by in situ hybridization to be localized within the stomium (Koltunow et al. 1990; Beals and Goldberg 1997). TA56 encodes a thiol endopeptidase (Beals and Goldberg 1997), while TA20 encodes a protein of unknown function (Goldberg et al. 1993; Beals and Goldberg 1997). Real-time qRT-PCR detected the presence of both sequences in stomium RNA, and indicated that TA20 mRNA was approximately 4-fold more prevalent than TA56 mRNA (Fig. 11C). Relative to internal rRNA standards, we estimated that TA20 and TA56 mRNAs represented approximately 1.4% and 0.4% of the stage +6 stomium mRNA population, or about 7,000 and 2,000 molecules per cell, respectively (Goldberg et al. 1978). These mRNA prevalences are consistent with those expected for mRNAs that can be detected within specific cell types using in situ hybridization procedures (Cox and Goldberg 1988). Together, these data show that LCM can be used successfully to capture stomium cells from the notch region of the anther and identify specific mRNAs.

Discussion

We characterized the differentiation and degeneration of the circular cell cluster and stomium during tobacco anther development using both light microscopy and TEM. These cell types form within the notch region of the anther and are required for dehiscence and release of pollen grains at flower opening (Fig. 1). Our major findings are summarized in Table 1 and a schematic representation of the cellular events that occur within the notch region at the level of the TEM is shown in Figure 12. Our results show that the stomium and circular cell cluster are specified early in phase 1 of anther development, following the differentiation of territories leading to locule formation. The circular cell cluster differentiates from L2 cells in the territory between the developing locules prior to the initiation of stomium differentiation and becomes a 12–14 cell specialized tissue containing calcium-oxalate crystals (Figs. 12; 13; Bonner and Dickinson 1989; Horner and Wagner 1992; D'Arcy et al. 1996). Thus, the L2 initials that give rise to

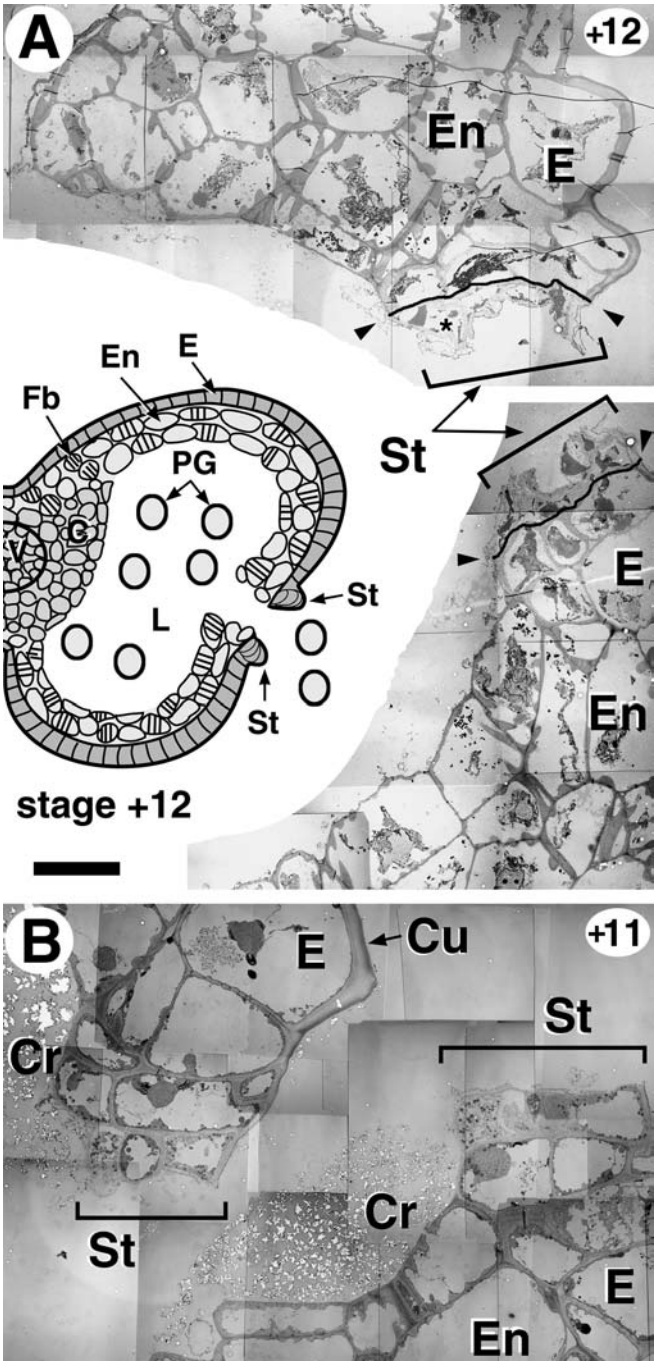

◀

Fig. 10A–B Stomium cell death and anther dehiscence. Anther sections from stages +11 and +12 were fixed and embedded in Spurr's epoxy resin as described in Materials and methods. Spurr's embedded anthers were sliced into ultra-thin sections and prepared for TEM. Anther developmental stages are shown in the top right corner. **A** Stage +12. Complete notch region of the split stomium shown in Fig. 9H. After breakage at the stomium, the two halves of the anther wall separate from each other. These two halves have been placed in close proximity to each other for this figure. The *asterisk* indicates the stomium cell highlighted in Fig. 7. The cartoon *inset* of a stage +12 anther theca represents the role of stomium breakage in pollen release. The *black border* and the *arrowheads* delineate the stomium cells from the other cells of the dehisced anther. *Brackets* highlight the two halves of the stomium that split at dehiscence. **B** Split notch region from a stage +11 anther that was mechanically sheared prior to fixation. *Brackets* highlight the two halves of the mechanically split stomium. *C* Connective, *Cr* calcium oxalate crystals, *Cu* cuticle, *E* epidermis, *En* endothecium, *Fb* Fibrous bands, *L* locule region in a bilocular anther, *PG* pollen grain, *St* stomium, *V* vascular region. *Bar* **A** 20 μm (scale for the TEM micrographs in both **A** and **B**)

the circular cell cluster are within a different region of the primordium than those that generate the archesporial cells (Figs. 12; 13). The stomium, in contrast, is specified from L1 cells contiguous to the circular-cell-cluster initials, and differentiates into a multi-tiered 9–12 cell structure after the circular cell cluster has begun to degenerate (Figs. 12; 13; Table 1).

Both the circular cell cluster and the stomium undergo a cell-death program and degenerate during phase 2 of anther development, although the timing differs (Figs. 1; 12; Table 1). The circular cell cluster degenerates first, contributing to the formation of a bilocular anther, while stomium degeneration occurs just prior to flower opening and provides a longitudinal slit for pollen release along each theca of the anther (Figs. 1, 12). These degeneration events occur independently of phase 2 developmental processes that take place within the locules (e.g., pollen differentiation, tapetum degeneration; Fig. 1), because male-sterile mutants obtained from either genetic screens (Kaul 1988; Dawson et al. 1993; Sanders et al. 1999) or the targeted ablation of the tapetum with cytotoxic genes (e.g., *TA29/barnase*, *TA29/diptheria toxin A*; Koltunow et al. 1990; Mariani et al. 1990) undergo normal dehiscence.

The TA56 thiol endopeptidase mRNA accumulation pattern reflects the sequential degeneration of the circular cell cluster and stomium—TA56 mRNA accumulates first in the circular cell cluster and then in the stomium (Fig. 11), and these events are under precise transcriptional control (Koltunow et al. 1990; Beals and Goldberg 1997). Other hydrolytic enzymes (e.g., cellulase) have been shown to be present in anthers just prior to dehiscence (del Campillo and Lewis 1992; Lashbrook et al. 1994; Neelam and Sexton 1995). In striking contrast with results obtained from tapetal cell ablation, targeted ablation of either the circular cell cluster and stomium or the stomium alone with a *TA56/barnase* gene late in anther development leads to anthers that fail to dehisce (Beals and Goldberg 1997). Collectively, these findings indicate that temporally-regulated cellular processes involving specific gene sets are required for anther dehiscence.

Coordinated events within several different cell types are required for anther dehiscence

In addition to the circular cell cluster and stomium, the endothecium and connective both play a major role in anther dehiscence (Keijzer 1987; Bonner and Dickinson 1989; Manning 1996). Like the circular cell cluster, the

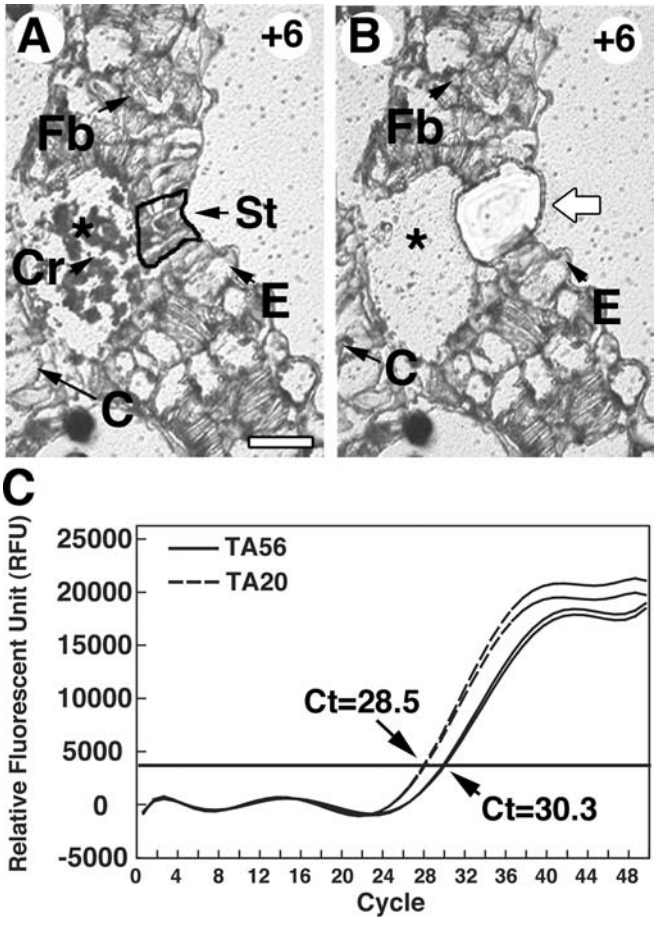

Fig. 11A–C Using laser capture microdissection (LCM) to isolate stomium cells and detect specific mRNAs. Stage +6 anthers were fixed, embedded in Paraplast, sliced into 10 μm transverse sections, and de-paraffinized with two washes of xylene before LCM (see Materials and methods). **A**, **B** Bright-field photographs of stage +6 anther notch region before and after LCM. **A** Notch region before LCM; *black outline* stomium cells marked for LCM. **B** Notch region after LCM; *asterisks* space previously occupied by the degenerated circular cell cluster (see Fig. 6), *large white arrow* hole left in the anther section after LCM of stomium cells. The calcium oxalate crystals present in **A** were scattered and lost during LCM. **C** Real-time quantitative reverse transcription-polymerase chain reaction (qRT-PCR) analysis of stomium mRNAs using TA56 and TA20 primers as outlined in Materials and methods. *Horizontal line* Ct, or PCR threshold value, calibrated relative to known amounts of plasmid DNA standards (data not shown). Curves show replica qRT-PCR reactions for each primer pair; *Ct* average value (standard deviation <0.2 Ct). The amount of PCR product varies according to the function $2^{[\Delta Ct]}$, where ΔCt is the absolute difference in Ct values. A ΔCt of 1 represents a 2-fold difference in the amount of PCR product. *C* Connective tissue, *Cr* calcium oxalate crystals, *E* epidermis, *Fb* fibrous bands, *P* pollen, *St* stomium. *Bar* **A** 50 μm (scale for **B**)

endothecium is derived from L2 layer cells of the anther primordium, but from a different territory (Fig. 13). Endothecial cells generate wall thickenings, or fibrous bands, during phase 2 of anther development (Figs. 1; 9D,F; 13; Table 1) Endothecial wall thickenings are composed of lignin and have been proposed to serve as a "spring" that flips the anther wall layers apart after stomium breakage (Keijzer 1987; Bonner and Dickinson 1989; Manning 1996). Fibrous bands within the endothecium are required for dehiscence, because an *A. thaliana* male-sterile mutant (*ms55*) that lacks endothecial wall thickenings due to a defect in the *MYB26* gene fails to dehisce (Dawson et al. 1999; Steiner-Lange et al. 2003). The connective, derived from the L3 primordium cell layer, also generates wall thickenings during phase 2 of tobacco anther development (Figs. 6D, H; 9H; 10A; 13). Degeneration of the connective, in addition to the circular cell cluster, establishes a confluent pollen chamber within each theca allowing the pollen grains to exit through a single opening (Fig. 1; Koltunow et al. 1990; Beals and Goldberg 1997). We showed previously that the *A. thaliana non-dehiscence1* mutant fails to undergo dehiscence as a consequence of premature connective cell death, indicating the importance of these cells, either directly or indirectly, in pollen release (Sanders et al. 1999).

The differentiation and specialization of diverse anther cell types required for dehiscence and pollen release are highly coordinated events that are timed precisely during floral development and scheduled to be completed when the flower opens (Fig. 13). The dehiscence program begins with the specification of cell types within the anther primordium (e.g., circular cell cluster, stomium, endothecium) and ends with breakage of the stomium within the anther wall and pollen release at flower opening (Fig. 13, Table 1). Thus, dehiscence requires a continuum of programmed events during both phase 1 and phase 2 of anther development. How cells required for dehiscence become specified within the L1, L2, and L3 layers of the anther primordium, and what genes and cellular processes guide their specialization during anther development remain major unanswered questions.

The anther dehiscence program is similar in tobacco and *A. thaliana*

Experiments with the anthers of related solanaceous plants (e.g., tomato, Bonner and Dickinson 1989; sweet pepper, Horner and Wagner 1980, 1992) have shown that similar events occur—a calcium-oxalate-filled circular cell cluster differentiates and degenerates, followed by the formation of a multi-tiered stomium that breaks at flower opening. The presence of a circular cell cluster filled with calcium oxalate druse crystals is a feature of solanaceous anthers (D'Arcy et al. 1996), and has been shown recently to enhance the pollination process by supplying calcium ions (Iwano et al. 2004).

Recently, we characterized anther development and the dehiscence program in *A. thaliana* (Sanders et al. 1999, 2000). A comparison of notch-region development and dehiscence in tobacco and *A. thaliana* is summarized in Table 2 and shows the remarkable conservation of precisely timed developmental events leading to pollen release in these divergent plant species. In *A. thaliana*, a small number of septum cells (two or three) differentiates

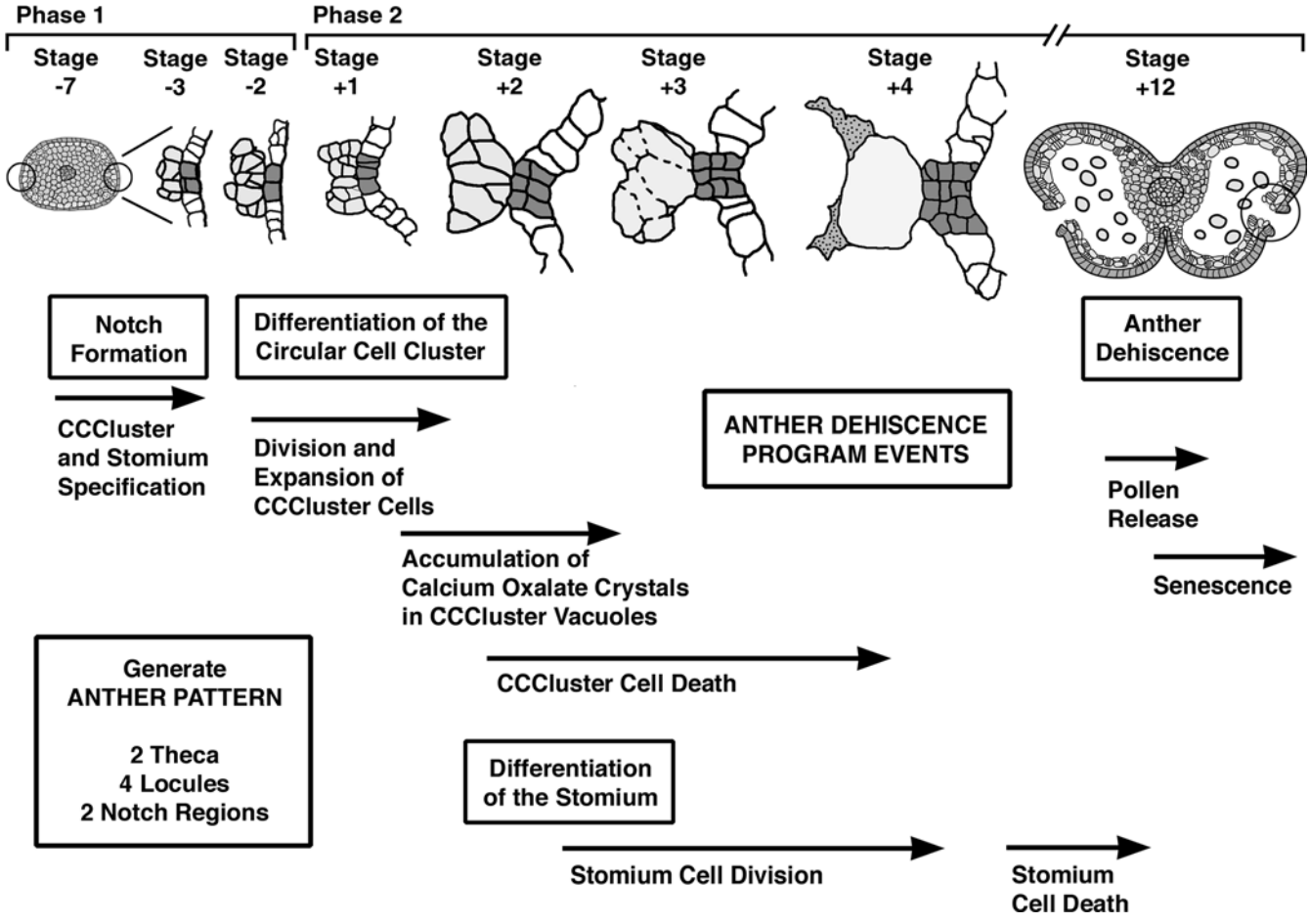

Fig. 12 Summary of events that occur during tobacco anther notch-region development. Notch-region cartoons were drawn from the TEM images shown in Figs. 3 and 6. Slight variation in notch-region development occurs within an anther (i.e., position of transverse section) and from anther to anther. The cells outlined in the cartoons (stages −3 to +4) represent the stomium (*dark shading*), circular cell cluster (*light shading*) and epidermis (*white*). At stage +4 the initial degeneration of connective cells is shown as a *speckled region*. The stage −7 primordium and stage +12 anther cartoons were taken from Fig. 1. *CCCluster* Circular cell cluster

in the notch region from sub-epidermal cells and degenerates midway through phase 2, creating a bilocular anther (Table 2; Sanders et al. 2000). The connective does not degenerate in *A. thaliana*, but does accumulate fibrous bands (Table 2; Sanders et al. 1999). The septum functions similarly to the circular cell cluster, but is simpler in structure, does not accumulate calcium oxalate crystals, and resides at the intersection of two round locules, in contrast with the U-shaped pollen sacs in tobacco (Fig. 1). Following septum degeneration, the stomium becomes visible within the notch region and degenerates just as the flower opens leading to pollen release (Table 2; Sanders et al. 1999, 2000). The *A. thaliana* stomium is also simpler than that observed in tobacco, consisting of only three cells that reside within a single epidermal layer of the notch region (Table 2; Sanders et al. 2000). Cellular events leading to the differentiation and degeneration of the circular cell cluster/septum and stomium are conserved, because a *TA56/GUS* reporter gene shows the same notch-region transcriptional specificity in *A. thaliana* as it does in tobacco. That is, the *TA56/GUS* gene is transcribed specifically within septum and stomium during phase 2 of anther development (Sanders 2000; P.M. Sanders and R.B. Goldberg, unpublished results). This suggests that the regulatory networks responsible for activating genes required for carrying out specialized dehiscence functions within the circular cell cluster/septum and stomium are ancient and evolved with the emergence of flowering plants.

What controls the specification of the notch region in the territory between the two locules?

How does the notch region form within the territory between the two locules, and how do the L1 and L2 cells within this territory become specified to follow stomium and circular cell cluster differentiation pathways? Figure 14 presents two alternative mechanisms by which these specification events might occur. Mechanism 1 proposes that the notch region forms autonomously during early phase 1 of anther development and that the L1 and L2 cells within this territory are pre-programmed to follow stomium and circular cell cluster pathways

Table 2 Comparison of anther notch region development and the dehiscence program in tobacco and *Arabidopsis thaliana*

Tobacco[a]		*A.thaliana*[a]	
Stage[b]	Major events in notch development	Stage[c]	Major events in notch development
−7 to −5	Anther pattern is generated from the stamen primordia. U-Shaped locules are derived from archesporial cell lineages. Expansion of the two locules in each theca creates the anther notch region	1–5	Anther pattern is generated from the stamen primordia. Round locules are derived from archesporial cell lineages. Expansion of the 2 locules in each theca creates the anther notch region
−5 to −1	CCC and stomium are specified within the notch region. CCC differentiates prior to the stomium	6–9	Septum and stomium are specified within the notch region[d]
+1	Meiosis complete within locules and tetrads present. End of phase 1 and beginning of phase 2	7	Meiosis complete within locules and tetrads present. End of phase 1 and beginning of phase 2
+1 to +2	CCC differentiation and division occur and calcium oxalate crystals accumulate	10	Septum cells present within notch region. Calcium oxalate crystals do not form
+2 to +4	CCC degeneration occurs. Stomium differentiation and division generate a multi-tiered structure with 9–12 cells	11	Expansion of endothecium cells occurs. Fibrous bands deposited in endothecium and connective cells
+3 to +5	Expansion of the endothecium and connectiveand deposition of fibrous bands. Connective degeneration leads to a bilocular anther	12	Septum cells degenerate and lead to a bilocular anther. A 3-celled, single-layered stomium is observed. Connective does not degenerate
+12	Degeneration of stomium creates break in anther wall and dehiscence/pollen release occurs. End of phase 2	13	Degeneration of stomium creates break in anther wall and dehiscence/pollen release occurs. End of phase 2

[a]Tobacco and *A. thaliana* have anthers with a 4 locule structure consisting of 2 locules per theca and a stomium between the 2 locules (1 theca → 2 locules → 1 stomium; see Fig. 1)
[b]Tobacco anther developmental stages were taken from Koltunow et al. (1990). Phase 1, stages −7 to −1; Phase 2 stages +1 to +12. Table 1 details the major events in tobacco anther development and notch region development
[c]*A. thaliana* anther developmental stages taken from Sanders et al. (1999). Phase 1, stages 1–8; Phase 2 stages 7–13
[d]Septum cells in *A. thaliana* analogous in position and function to CCC of tobacco, although septum cells do not accumulate calcium oxalate crystals. The anther developmental stage(s) at which septum and stomium cells differentiate in *A. thaliana* is not known; however, septum and stomium cells are present at stages 10 and 12, respectively (Sanders et al. 1999, 2000). Septum differentiation and degeneration occur before similar events take place in the stomium (Sanders et al. 1999, 2000), analogous to what occurs in tobacco for the CCC and stomium (Table 1)

(Davidson 1991). Mechanism 2, in contrast, hypothesizes that notch region specification is dependent upon signals generated by the differentiating locules. These signals are transmitted obliquely from each locule and, at their intersection, enable stomium and circular cell cluster initials to be specified from receptive L1 and L2 cells (Fig. 14), i.e., stomium and circular cell cluster L1 and L2 founder cells are conditionally specified as a consequence of their position between the two differentiating locules (Davidson 1991). One corollary to mechanism 2 is that L1 or L2 cells on the periphery of the anther primordium should have the potential to differentiate into a stomium or circular cell cluster, respectively, provided the relevant signals are present. Mechanism 1 predicts that altering the number and/or position of locules within each theca should have no effect on notch region development. In contrast, mechanism 2 predicts that alterations in the pattern of locules within the anther should affect notch-region development and dehiscence.

We used mutant *A. thaliana aintegumenta* and *ettin* anthers to show that notch region development and dehiscence are dependent upon the formation of two contiguous locules (Sanders 2000; P.M. Sanders, Y. Mizukami, R.L. Fischer, and R.B. Goldberg, unpublished observations). Mutations in either the *AINTEGUMENTA* (*ANT*) gene that encodes an AP2-class transcription factor (Elliot et al. 1996; Klucher et al. 1996) or the *ETTIN* (*ETT*) gene that encodes an auxin-response-element transcription factor (Sessions et al. 1997) affect both the position and number of locules within the anther (Sessions et al. 1997). We observed that septum and stomium cell differentiation occurs only at the intersection between two locules, regardless of where these locules are positioned within the anther (Sanders 2000; P.M. Sanders, Y. Mizukami, R.L. Fischer, and R.B. Goldberg, unpublished observations). Notch region formation and dehiscence do not occur within either an anther or theca containing only a single locule (Sanders 2000; P.M. Sanders, Y. Mizukami, R.L. Fischer, and R.B. Goldberg, unpublished observations).

Experiments with *A. thaliana* fertility mutants that have a defect in the *SPOROCYTELESS/NOZZLE* MADS-box transcription factor gene (Schiefthaler et al. 1999; Yang et al. 1999) support this conclusion. Archesporial cells do not differentiate in *sporocyteless/nozzle*

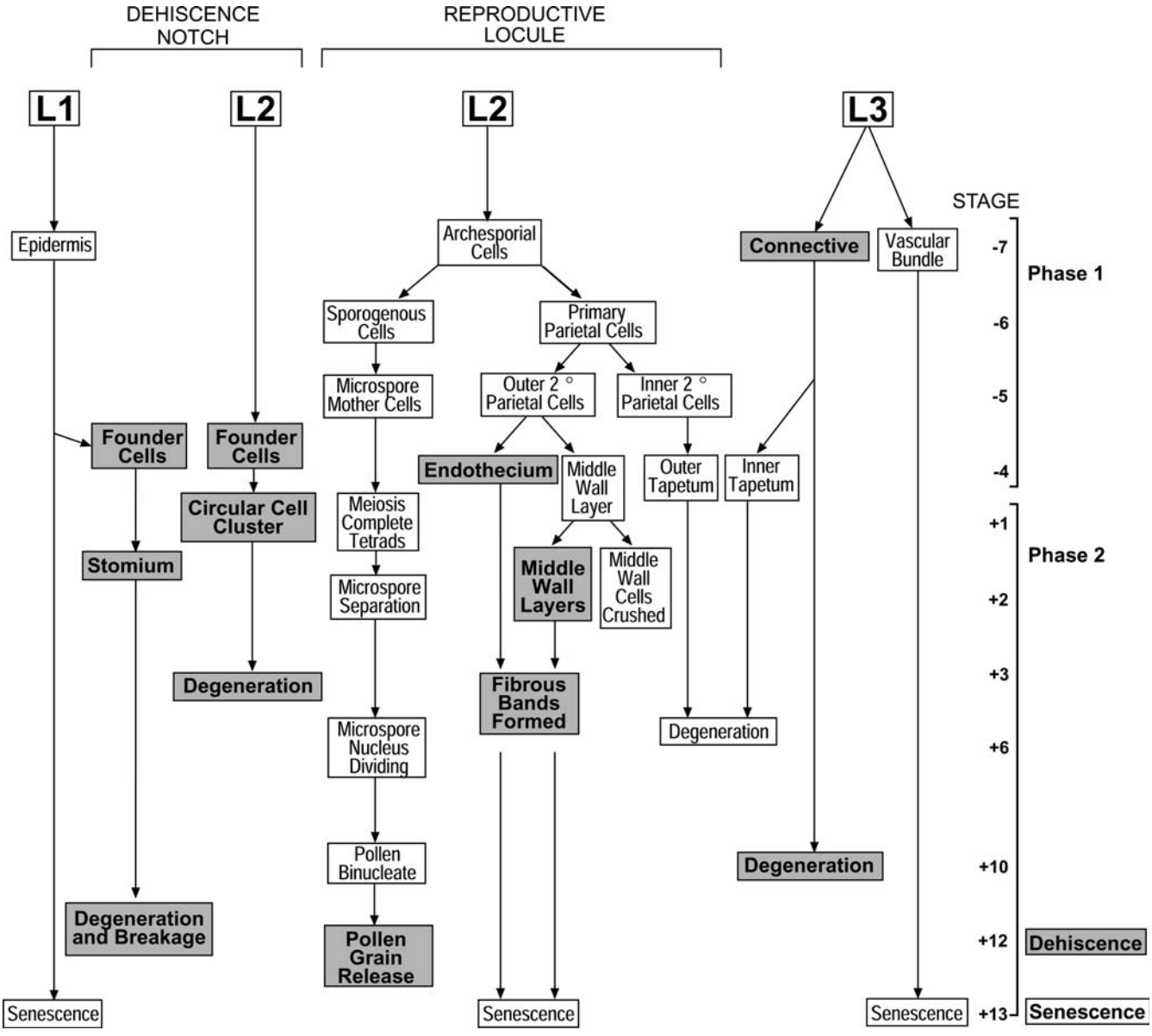

Fig. 13 Cell lineages participating in tobacco anther dehiscence. Stages at which dehiscence events occur within specific cell types were taken from the results reported in this paper (Table 1). Stages at which other developmental events occur were taken from our previous studies (Koltunow et al. 1990). Cells derived from L1, L2, and L3 primordium layers were based upon the experiments presented here (circular cell cluster, stomium), those reported previously from our laboratory (Koltunow et al. 1990), and the histological studies of Satina and Blakeslee (1941) and Joshi et al. (1967). Middle wall-layer lineage is based upon Davis (1966). Cells of the inner tapetum can originate from both the L2 and L3 layers (Hill and Malmberg 1996). The *bold lettering* and *shaded boxes* represent cell types and events that are part of the anther dehiscence program. Adapted from Goldberg et al. (1993, 1995)

anther primordia, and, as a consequence, fail to differentiate pollen-containing locules and associated wall layers (e.g., tapetum, endothecium). *Sporocyteless*/*nozzle* anthers also do not contain septum and stomium cells within their rudimentary notch region, even though differentiated epidermal and connective-like sub-epidermal cells are present (Yang et al. 1999). This is consistent with the studies reported here, which show that histological changes within the notch region become apparent only after the locules have begun to differentiate (Fig. 3). Together, these results suggest strongly that the differentiation of the notch region is dependent upon signals generated by two locules within each theca (Fig. 14, mechanism 2). What these signals are, which cells produce them, and how they interact with L1 and L2 cells in the interlocular region to induce stomium and circular cell cluster/septum specification events remain to be determined.

Do the circular cell cluster and stomium differentiate independently of each other within the notch region?

Do cells of the circular cell cluster and stomium interact with each other during anther development and what

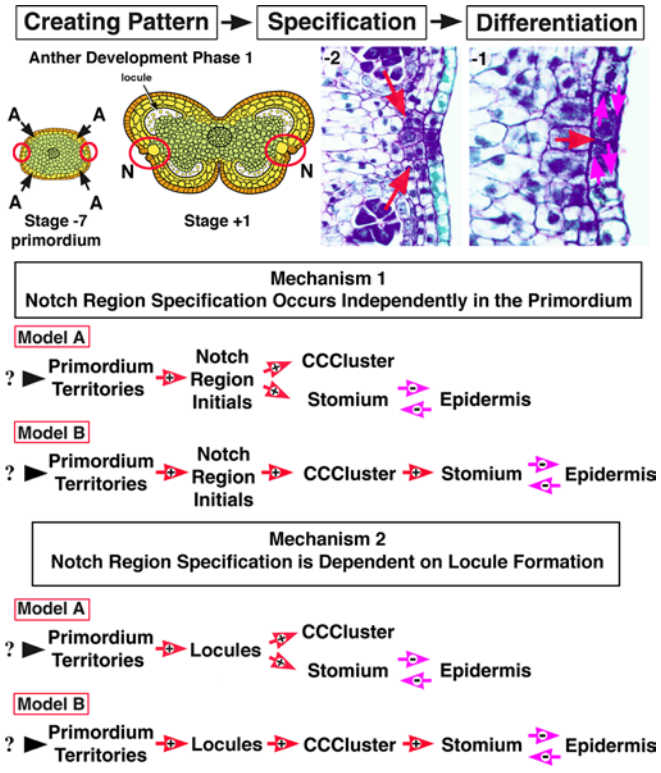

Fig. 14 Models for the specification and differentiation of the circular cell cluster and stomium. The cartoons for stage −7 and +1 anthers were taken from Fig. 1. The *red circles* at stage −7 highlight the region in the primordium that will become the notch region, as seen at stage +1. The *arrows* at stage −7 designate the territories of the four archesporial cell regions that will develop into the locules, as seen in stage +1. The bright-field photographs show the notch region of stage −2 and stage −1 anthers and were taken from Fig. 3. *Arrows* with a + sign indicate positive interactions, while *arrows* with a − sign indicate negative interactions. Individual arrows are conceptual and do not reflect the possible number of interactions, molecules, and/or pathways responsible for each step. *A* Archesporial cell territories, *CCCluster* circular cell cluster, *N* notch

defines the boundary of the notch region? Two models for stomium and circular cell cluster differentiation are presented in Figure 14, both of which are dependent upon signaling for the initial specification of the notch region (mechanism 2). In model A, the stomium and circular cell cluster differentiate independently of each other after their L1 and L2 founder cells are specified by a common signaling mechanism. Alternatively, model B proposes that stomium differentiation is dependent upon signals generated by contiguous cells of the circular cell cluster. This model assumes that circular cell cluster development is required before stomium differentiation and division can occur (Fig. 12), and that pre-stomium initials require signals in addition to those obtained from the locules in order to undergo a differentiation pathway. Both models propose that negative interactions (e.g., between the stomium and epidermal neighbors) limit the size of the notch region and define its boundary (Fig. 14; Larkin et al. 2003). Signals between the circular cell cluster and stomium or the stomium and epidermal cells could be transmitted by plasmodesmata connections (Fig. 8; Haywood et al. 2002), more conventional ligand/receptor pathways (Larkin et al. 2003), or both.

At the present time we do not know which model is correct or whether interactions occur between stomium and adjacent epidermal cells. The circular cell cluster differentiates and divides from stages −4 to +2, whereas analogous stomium events occur later, during stages +1 to +4, while the circular cell cluster is degenerating (Fig. 12; Table 1). Stomium differentiation is completed after the circular cell cluster has disappeared, and stomium cell death occurs in the absence of a circular cell cluster (Fig. 12; Table 1). Thus, the circular cell cluster is not required for cellular processes that occur within the stomium during most of phase 2 of anther development (Fig. 12, stages +4 to +12; Table 1). These observations are consistent with the hypothesis that the circular cell cluster and stomium differentiate and function independently of each other after they are specified within the primordium interlocular region (Fig. 14, model B).

One way to test these models is to use targeted cell ablation studies (Mariani et al. 1990; Koltunow et al. 1990; Goldberg et al. 1995; Beals and Goldberg 1997) to selectively eliminate either the circular cell cluster or the stomium during phase 1 of anther development (Fig. 1). For example, if model B is correct, then destruction of the circular cell cluster will have no affect on stomium differentiation. Conversely, ablation of the stomium will not affect circular cell cluster formation. The absence of the stomium, however, might induce contiguous epidermal cells to enter a stomium differentiation pathway due to the elimination of negative signals (Fig. 14). The ability to use LCM methods (Kerk et al. 2003) to isolate cells from the circular cell cluster and stomium at any stage in their development opens the door for identifying cell-specific genes and promoters that can be used drive the ablation process (Fig. 11).

What coordinates cellular events within the circular cell cluster and stomium with other developmental processes within the flower?

The developmental processes that occur within the notch region must be coordinated with other events that occur within the anther (Goldberg et al. 1993). For example, pollen grain formation, tapetal cell degeneration, expansion of wall and epidermal layers, deposition of fibrous bands in the connective and endothecium, and connective cell degeneration need to be synchronized with the differentiation and degeneration of the circular cell cluster and stomium (Fig. 13; Table 1). In addition, anther development and dehiscence must be timed with events that occur within other floral organs (i.e., sepals, petals, pistil) so that successful pollination and fertilization can take place when the flower opens.

Clues to what controls the timing of anther dehiscence come from studies with late-dehiscence mutants and genes involved in hormone activity. *A. thaliana*

mutants that are defective in either JA biosynthesis (e.g., *dde1*/*opr3*, *dde2*/*allene oxidase synthase*, *dad1*) or perception (e.g., *coi1*) are male sterile and have anthers that dehisce too late for successful pollination to occur (Feys et al. 1994; McConn and Browse 1996; Sanders et al. 2000; Stintzi and Browse 2000; Ishiguro et al. 2001; Park et al. 2002; Von Malek et al. 2002). For example, *dde1*/*opr3* plants lack 12-oxophytodienoate reductase, an enzyme in the JA biosynthetic pathway (Sanders et al. 2000; Stintzi and Browse 2000). The stomium and septum differentiate normally in *dde1*/*opr3* anthers, but stomium degeneration is delayed, indicating that JA is an important signal for controlling the timing of stomium breakage and anther dehiscence (Sanders et al. 2000). Other hormones, such as ethylene, auxin, and GA, have also been shown to play a role in anther dehiscence. Inhibiting the *etr1-1 ethylene receptor* gene (Rieu et al. 2003) or increasing auxin sensitivity by *Agrobacterium tumefaciens rolB* gene over-expression (Cecchetti et al. 2004) generates a late-dehiscence phenotype in transgenic tobacco plants analogous to that observed in *dde1*/*opr3* anthers (Sanders et al. 2000; Stintzi and Browse 2000). In addition, overexpressing the *HvGAMYB* gene in barley, a GA-induced transcriptional regulator, leads to anthers that fail to dehisce (Murray et al. 2003), perhaps acting in cooperation with a microRNA (Achard et al. 2004). Together, these studies indicate that a complex set of hormonal interactions is required, in part, to coordinate events within the flower leading to anther dehiscence. How this occurs, as well as the molecular processes and genes that control the differentiation and degeneration of cells required for anther dehiscence, remains to be determined.

Acknowledgements We thank Birgitta Sjostrand for her expertise and help with the TEM studies, Sharon Hue Tu for assistance taking the TEM pictures, and Layla Maloff for teaching us how to use the Leica Laser Capture Microdissection System. We also thank Lynne Olson and Reed Hutchinson at the OID Digital Imaging Facility at the UCLA Center for Health Sciences for help in the preparation of figures. This work was funded by NSF and HHMI grants to R.B.G.

References

Achard P, Herr A, Baulcombe DC, Harberd NP (2004) Modulation of floral development by a gibberellin-regulated microRNA. Development 131:3357–3365

Asano T, Masumura T, Kusano H, Kikuchi S, Kurita A, Shimata H, Kadowaki K-i (2002) Construction of a specialized cDNA library from plant cells isolated by laser capture microdissection: toward comprehensive analysis of the genes expressed in the rice phloem. Plant J 32:401–408

Beals TP, Goldberg RB (1997) A novel cell ablation strategy blocks tobacco anther dehiscence. Plant Cell 9:1527–1545

Bonner LJ, Dickinson HG (1989) Anther dehiscence in *Lycopersicon esculentum* Mill. I. Structural aspects. New Phytol 113:97–115

Botha CEJ, Hartley BJ, Cross RHM (1993) The ultrastructure and computer-enhanced digital image analysis of plasmodesmata at the Kranz mesophyll-bundle sheath interface of *Themeda triandra* var. imberbis (Retz) A. Camus in conventionally-fixed leaf blades. Ann Bot 72:255–261

Campillo E del, Lewis LN (1992) Occurrence of 9.5 cellulase and other hydrolases in flower reproductive organs undergoing major cell wall disruption. Plant Physiol 99:1015–1020

Cecchetti V, Pomponi M, Altamura MM, Pezzotti M, Marsilio S, D'Angeli SD, Tornielli GB, Constantino P, Cardarelli M (2004) Expression of *rolB* in tobacco flowers affects the coordinated processes of anther dehiscence and style elongation. Plant J 38:512–525

Cox KH, Goldberg RB (1988) Analysis of gene expression. In: Shaw CH (ed) Plant molecular biology: a practical approach. IRL Press, Oxford, pp 1–34

D'Arcy WG (1996) Anthers and stamens and what they do. In: D'Arcy WG, Keating RC (eds) The anther: form, function and phylogeny. Cambridge University Press, Cambridge, pp 1–24

D'Arcy WG, Keating RC, Buchmann SL (1996) The calcium oxalate package or so-called resorption tissue in some angiosperm anthers. In: D'Arcy WG, Keating RC (eds) The anther: form, function and phylogeny. Cambridge University Press, Cambridge, pp 159–191

Davidson EH (1991) Spatial mechanisms of gene regulation in metazoan embryos. Development 113:1–26

Davis GL (1966) Systematic embryology of the angiosperms. Wiley, New York

Dawson J, Wilson ZA, Aarts MGM, Braithwaite AF, Briarty LG, Mulligan BJ (1993) Microspore and pollen development in six male-sterile mutants of *Arabidopsis thaliana*. Can J Bot 71:629–638

Dawson J, Sözen E, Vizir I, Waeyenberge SV, Wilson ZA, Mulligan BJ (1999) Characterization and genetic mapping of a mutation (*ms35*) which prevents anther dehiscence in *Arabidopsis thaliana* by affecting secondary wall thickening in the endothecium. New Phytol 144:213–222

Elliott RC, Betzner AS, Huttner E, Oakes MP, Tucker WQ, Gerentes D, Perez P, Smyth DR (1996) *AINTEGUMENTA*, an *APETALA2*-like gene of *Arabidopsis* with pleiotropic roles in ovule development and floral organ growth. Plant Cell 8:155–168

Feys BJ, Benedetti CE, Penfold CN, Turner JG (1994) *Arabidopsis* mutants selected for resistance to the phytotoxin coronatine are male sterile, insensitive to methyl jasmonate, and resistant to a bacterial pathogen. Plant Cell 6:751–759

Goldberg RB, Hoschek G, Kamalay JC, Timberlake WE (1978) Sequence complexity of nuclear and polysomal RNA in leaves of the tobacco plant. Cell 14:123–131

Goldberg RB, Beals TP, Sanders PM (1993) Anther development: basic principles and practical applications. Plant Cell 5:1217–1229

Goldberg RB, Sanders PM, Beals TP (1995) A novel cell-ablation strategy for studying plant development. Phil Trans R Soc Lond B 350:5–17

Haywood V, Kragler F, Lucas WJ (2002) Plasmodesmata: pathways for protein and ribonucleoprotein signaling. Plant Cell 14 [Suppl]:S303–S325

Hill JP, Malmberg RL (1996) Timing of morphological and histological development in premeiotic anthers of *Nicotiana tabacum* cv. Xanthi (Solanaceae). Am J Bot 83:285–295

Horner HT, Wagner BL (1980) The association of druse crystals with the developing stomium of *Capsicum annuum* (Solanaceae) anthers. Am J Bot 67:1347–1360

Horner HT, Wagner BL (1992) Association of four different calcium crystals in the anther connective tissue and hypodermal stomium of *Capsicum annuum* (Solanaceae) during microsporogenesis. Am J Bot 79:531–541

Ishiguro S, Kawai-Oda A, Ueda J, Nishida I, Okada K (2001) The *DEFECTIVE IN ANTHER DEHISCHENCE1* gene encodes a novel phospholipase A1 catalyzing the initial step of jasmonic acid biosynthesis, which synchronizes pollen maturation, anther dehiscence, and flow opening in *Arabidopsis*. Plant Cell 13:2191–2209

Iwano M, Tetsuyuki E, Shiba H, Takayama S, Isogai A (2004) Calcium crystals in the anther of *Petunia*: the existence and biological significance in the pollination process. Plant Cell Physiol 45:40–47

Joshi PC, Wadhwani AM, Johri BM (1967) Morphological and embryological studies of *Gossypium*. Proc Natl Inst Sci India 33:37–93

Kaul MLH (1988) Male sterility in higher plants. Springer, Berlin Heidelberg New York

Keijzer CJ (1987) The process of anther dehiscence and pollen dispersal. I. The opening mechanism of longitudinally dehiscing anthers. New Phytol 105:487–498

Kerk NM, Ceserani T, Tausta SL, Sussex IM, Nelson TM (2003) Laser capture microdissection of cells from plant tissues. Plant Physiol 132:27–35

Klucher KM, Chow H, Reiser L, Fischer RL (1996) The *AINTEGUMENTA* gene of *Arabidopsis* required for ovule and female gametophyte development is related to the floral homeotic gene *APETALA2*. Plant Cell 8:137–153

Koltunow AM, Truettner J, Cox KH, Wallroth M, Goldberg RB (1990) Different temporal and spatial gene expression patterns occur during anther development. Plant Cell 2:1201–1224

Larkin JC, Brown ML, Schiefelbein J (2003) How do cells know what they want to be when they grow up? Lessons from epidermal patterning in *Arabidopsis*. Annu Rev Plant Biol 54:403–430

Lashbrook CC, Gonzalez-Bosch C, Bennett AB (1994) Two divergent endo-β-1,4-glucanase genes exhibit overlapping expression in ripening fruit and abscising flowers. Plant Cell 6:1485–1493

Manning JC (1996) Diversity of endothecial patterns in the angiosperms. In: D'Arcy WG, Keating RC (eds) The anther: form, function and phylogeny. Cambridge University Press, Cambridge, pp 136–158

Mariani C, De Beuckeleer M, Truettner J, Leemans J, Goldberg RB (1990) Induction of male sterility in plants by a chimeric ribonuclease gene. Nature 347:737–741

McConn M, Browse J (1996) The critical requirement for linolenic acid is pollen development, not photosynthesis, in an *Arabidopsis* mutant. Plant Cell 8:403–416

Murray F, Kalla R, Jacobsen J, Gubler F (2003) A role for HvGMYB in anther development. Plant J 33:481–491

Nakazano M, Qui F, Borsuk L, Schnable PS (2003) Laser capture microdissection, a tool for the global analysis of gene expression in specific plant cell types: identification of genes expressed differentially in epidermal cells or vascular cells. Plant Cell 15:1–15

Neelam A, Sexton R (1995) Cellulase (endo β-1,4 glucanase) and cell wall breakdown during anther development in sweet pea (*Lathyrus odoratus* L.): isolation and characterization of partial cDNA clones. J Plant Physiol 146:622–628

Park J-H, Halitschike R, Kim HB, Baldwin IT, Feldmann KA, Feyereisen R (2002) A knock-out mutation in allele oxidase synthase results in male sterility and defective wound signal transduction in *Arabidopsis* due to a block in jasmonic acid biosynthesis. Plant J 31:1–12

Park SK, Yoon YH, Kim BC, Hwang YH, Chung IK, Nam HG, Kim DU (1996) Pollen of a male-sterile mutant of *Arabidopsis thaliana* isolated from a T-DNA insertion pool is not effectively released from the anther locule. Plant Cell Physiol 37:580–585

Rieu I, Wolters-Arts M, Derksen J, Mariani C, Weterings K (2003) Ethylene regulates the timing of anther dehiscence in tobacco. Planta 217:131–137

Sanders PM (2000) Anther dehiscence: genetic and molecular characterization. Ph.D. Dissertation, University of California, Los Angeles, ISBN 0–599–61025–5, UMI Abstract ATT 9957828 (http://wwwlib.umi.com/dissertations/fullcit/9957828)

Sanders PM, Bui AQ, Weterings K, McIntire KN, Hsu YC, Lee PY, Truong MT, Beals TP, Goldberg RB (1999) Anther developmental defects in *Arabidopsis thaliana* male-sterile mutants. Sex Plant Reprod 11:297–322

Sanders PM, Lee PY, Biegsen C, Boone JD, Beals TP, Weiler EW, Goldberg RB (2000) The *Arabidopsis DELAYED DEHISCENCE1* gene encodes an enzyme in the jasmonic acid synthesis pathway. Plant Cell 12:1041–1062

Satina S, Blakeslee AF (1941) Periclinal chimeras in *Datura stramonium* in relation to development of leaf and flower. Am J Bot 28:862–871

Schiefthaler U, Balasubramanian S, Sieber P, Chevalier D, Wisman E, Schneitz K (1999) Molecular analysis of *NOZZLE*, a gene involved in pattern formation and early sporogenesis during sex organ development in *Arabidopsis thaliana*. Proc Natl Acad Sci USA 96:11664–11669

Scott RJ, Spielman M, Dickinson HJ (2004) Stamen structure and function. Plant Cell 16 [Suppl]:S46–S60

Sessions A, Nemhauser JL, McColl A, Roe JL, Feldmann KA, Zambryski PC (1997) *ETTIN* patterns the Arabidopsis floral meristem and reproductive organs. Development 124:4481–4491

Spurr AH (1969) A low viscosity epoxy resin embedding medium for electron microscopy. J Ultrastruct Res 26:31–43

Steiner-Lange S, Unte US, Eckstein L, Yang C, Wilson ZA, Schmeizer E, Dekker K, Saedler H (2003) Disruption of *Arabidopsis thaliana MYB26* results in male sterility due to non-dehiscent anthers. Plant J 34:519–528

Stintzi A, Browse J (2000) The *Arabidopsis* male sterile mutant, *opr3*, lacks the 12-oxophytodienoic acid reductase required for jasmonate biosynthesis. Proc Natl Acad Sci USA 97:10625–10630

Trull MC, Holaway BL, Friedman WE, Malmberg RL (1991) Developmentally regulated antigen associated with calcium crystals in tobacco anthers. Planta 186:13–16

Venkatesh CS (1957) The form, structure, and special ways of dehiscence of anthers of Cassia 3. Subgenus Senna. Phytomorphology 7:253–273

Von Malek B, van der Graaff E, Schneitz K Keller, B (2002) The *Arabidopsis* male-sterile mutant *dde2–2* is defective in the *ALLENE OXIDASE SYNTHASE* gene encoding one of the key enzymes of the jasmonic acid biosynthesis pathway. Planta 216:187–192

Yang WC, Ye D, Xu J, Sundaresan V (1999) The *SPOROCYTELESS* gene of *Arabidopsis* is required for initiation of sporogenesis and encodes a novel nuclear protein. Genes Dev 13:2108–2117